Couple stress in the vertex model of cellular monolayers

OEJ

January 4, 2022

Abstract

The vertex model is widely used to simulate the mechanical properties of epithelia and other multicellular tissues. This framework allows a Cauchy stress to be attributed to each cell, and its symmetric component has been widely reported, at least for planar monolayers. Here we consider the stress attributed to the neighbourhood of each cellular trijunction, deriving in particular its leading-order antisymmetric component and the associated couple stress, which can be used to characterise the degree to which individual cells resist in-plane bending deformations. We derive a corresponding torque constraint and the associated discrete scalar potentials (analogues of Airy and Mindlin stress functions), *which we use to visualise stress patterns in monolayers.*

1 Introduction

The vertex model is a powerful tool for describing the mechanics of spatially heterogeneous multicellular tissues [1, 2, 3, 4]. A planar epithelium, for example, is represented as polygons tiling a plane. A mechanical strain energy is attributed to each cell that is a function of geometric invariants (such as the cell's area and perimeter) and the total energy of the monolayer is minimised, at a rate defined via a model of viscous dissipation, by varying vertex locations, potentially allowing for cell neighbour exchanges (T1 transitions). A force balance at each vertex is defined by taking the first variation of each cell's mechanical energy with respect to vertex displacement. The changes of a cell's area and perimeter arising from displacement of its vertices define contributions to forces (and hence the mechanical stresses) attributed to each cell. The model has been used to predict a symmetric Cauchy stress tensor associated with each cell [5] that aligns with cell shape [6] and allows viscoelastic moduli for bulk and shear deformations to be evaluated [7].

In 2D continuum mechanics, it is often convenient to express the Cauchy stress in terms of a scalar potential, the Airy stress function. However in seeking to construct the discrete analogue of the Airy stress function, it has been shown [8] that the requirement for both forms of the Cauchy stress (that defined over cells, and that defined over the neighbourhood of cellular trijunctions) to be symmetric places severe geometric constraints on cell shape, specifically that cell edges should be orthogonal to links between cell centres and that each vertex should lie at the orthocentre of the triangle formed by its immediate neighbours. These constraints are not met in typical simulations. This discrepancy can be explained in part by noting that while forces balance at vertices in the normal implementation of the vertex model, torque balance is not enforced. Here we consider how the discrepancy can be accommodated by accounting for so-called couple stresses, which we derive explicitly, provided a weaker torque constraint is satisfied.

The Cauchy stress attributed to a cell (which hereafter we call the force stress, evaluated as the first spatial moment of the forces acting over a cell) can be partitioned into an isotropic component (defining an effective cell pressure) and a deviatoric component (describing the shear stress experienced by each cell) [6]. The couple stress provides an additional measure of the stress arising from in-plane bending effects. The couple stress contributes to asymmetries in the Cauchy stress and can be evaluated by considering second-order spatial gradients of a virtual tissue deformation. We show how the degree to which a cell is 'bent out of shape' can be evaluated in simple geometric terms. The calculation is facilitated through use of incidence matrices [8], which explicitly capture topological relationships between cell vertices, edges and faces and enable the primal network of polygonal cells to be related directly to the dual network, a triangulation connecting adjacent cell

centres. Incidence matrices also provide the building blocks of the discrete differential operators needed to represent stresses using potentials. Unlike the three operators needed for normal continuum mechanics (grad, div and curl), up to 16 different operators are required in the general instance when links between cell centres are not orthogonal to cell edges (in two spatial dimensions), which enable a Helmholtz decomposition to be exploited. *Visualisation of stress patterns* across the monolayer is achieved by derivation of the Airy stress function, supplemented with an additional stress function that is analogous to that defined by Mindlin for couple-stress materials [9].

2 The model

2.1 Couple stress in continua

In two dimensions, a continuous couple-stress material can be characterised by a force-stress tensor $\boldsymbol{\sigma}$ and couple-stress vector $\boldsymbol{\mu}$, with the antisymmetric component of $\boldsymbol{\sigma}$ expressed as a derivative of $\boldsymbol{\mu}$. There are three independent components of the symmetric component of force stress $\boldsymbol{\sigma}^{(s)} \equiv \frac{1}{2}(\boldsymbol{\sigma}+\boldsymbol{\sigma}^\top)$ and two of $\boldsymbol{\mu}$, constrained by two (scalar) force balances and a torque balance. These constraints are satisfied by expressing $\boldsymbol{\sigma}$ and $\boldsymbol{\mu}$ in terms of two potentials, the Airy stress function $\psi(\mathbf{x})$ plus a second stress function $\Psi(\mathbf{x})$ described by Mindlin [9], such that [10]

$$\sigma_{pq} = \varepsilon_{pr}\partial_r(\varepsilon_{qs}\partial_s\psi - \partial_q\Psi), \quad \mu_p = -\varepsilon_{pq}\partial_q\Psi, \tag{1}$$

ensuring that $\partial_p\sigma_{pq} = 0$ and $\partial_p\mu_p = 0$. Here $\boldsymbol{\varepsilon}$ is the 2D Levi-Civita tensor representing a clockwise $\pi/2$ rotation. Equivalently, in Cartesians,

$$\sigma_{xx} = \partial_y^2\psi - \partial_x\partial_y\Psi, \quad \sigma_{yy} = \partial_x^2\psi + \partial_x\partial_y\Psi, \quad \sigma_{xy} = -\partial_x\partial_y\psi - \partial_y^2\Psi, \quad \sigma_{yx} = -\partial_x\partial_y\psi + \partial_x^2\Psi \tag{2}$$

with $\mu_y = \partial_x\Psi$ and $-\mu_x = \partial_y\Psi$. This formulation makes no constitutive assumptions beyond material continuity. The Airy stress function determines the isotropic component of the force-stress via $\mathrm{Tr}(\boldsymbol{\sigma}) = \nabla^2\psi$, while the Mindlin stress function determines the antisymmetric force stress via $\boldsymbol{\sigma}^{(a)} \equiv \frac{1}{2}(\boldsymbol{\sigma} - \boldsymbol{\sigma}^\top) = -\frac{1}{2}\boldsymbol{\varepsilon}\nabla^2\Psi = -\frac{1}{2}\boldsymbol{\varepsilon}(\partial_x\mu_y - \partial_y\mu_x)$. The stress can be decomposed into isotropic, antisymmetric and symmetric-deviatoric parts as

$$\boldsymbol{\sigma} = \tfrac{1}{2}\mathsf{I}\nabla^2\psi - \tfrac{1}{2}\boldsymbol{\varepsilon}\nabla^2\Psi + \check{\boldsymbol{\sigma}}, \quad \check{\boldsymbol{\sigma}} \equiv \begin{pmatrix} \frac{1}{2}(\partial_y^2 - \partial_x^2)\psi - \partial_x\partial_y\Psi & -\partial_x\partial_y\psi - \frac{1}{2}(\partial_y^2 - \partial_x^2)\Psi \\ -\partial_x\partial_y\psi - \frac{1}{2}(\partial_y^2 - \partial_x^2)\Psi & \frac{1}{2}(\partial_x^2 - \partial_y^2)\psi + \partial_x\partial_y\Psi \end{pmatrix}, \tag{3}$$

where $\mathrm{Tr}(\check{\boldsymbol{\sigma}}) = 0$ and $\check{\boldsymbol{\sigma}} = \check{\boldsymbol{\sigma}}^\top$. $\check{\boldsymbol{\sigma}}$ has real eigenvalues $\pm\lambda$, with $\lambda \geq 0$ measuring shear, which depends on both ψ and Ψ via

$$\lambda = \sqrt{\left[\tfrac{1}{2}(\partial_y^2 - \partial_x^2)\psi - \partial_x\partial_y\Psi\right]^2 + \left[\partial_x\partial_y\psi + \tfrac{1}{2}(\partial_y^2 - \partial_x^2)\Psi\right]^2}. \tag{4}$$

For later reference, writing $\mathbf{h} = -\nabla\psi - \boldsymbol{\mu}$ implies that $\boldsymbol{\sigma} = -\frac{1}{2}\mathsf{I}\nabla\cdot\mathbf{h} + \frac{1}{2}\boldsymbol{\epsilon}\,\mathrm{curl}\,\mathbf{h} + \check{\boldsymbol{\sigma}}$ [*check*], and

$$\sigma_{pq} = \varepsilon_{pr}\partial_r(-\varepsilon_{qs}h_s). \tag{5}$$

ψ and Ψ can be regarded as the scalar potentials of the vector $\mathbf{h}$ in a Helmholtz decomposition.

The gradient of a smooth deformation $\mathbf{u}(\mathbf{x})$ can be decomposed into $\mathsf{E} + \mathsf{W}$, where $\mathsf{E} = \mathsf{E}^\top \equiv \frac{1}{2}(\nabla\mathbf{u} + \nabla\mathbf{u}^\top)$ represents strain and $\mathsf{W} \equiv \frac{1}{2}(\nabla\mathbf{u} - \nabla\mathbf{u}^\top) = \boldsymbol{\varepsilon}\omega$ is a rotation, where $\omega \equiv \frac{1}{2}\nabla\cdot(\boldsymbol{\varepsilon}\mathbf{u})$. Likewise, $\mathsf{M} \equiv (\nabla\otimes\nabla)\mathbf{u}$ can be deomposed as $\mathsf{M} = \nabla\mathsf{E} + \nabla\mathsf{W}$. M is symmetric in its first two arguments, while contracting over them gives

$$\mathsf{I} : \nabla\mathsf{E} = \tfrac{1}{2}(\nabla^2\mathbf{u} + \nabla(\nabla\cdot\mathbf{u})), \quad \mathsf{I} : \nabla\mathsf{W} = \tfrac{1}{2}(\nabla^2\mathbf{u} - \nabla(\nabla\cdot\mathbf{u})) \equiv -2\boldsymbol{\kappa}, \tag{6}$$

which defines a curvature vector $\boldsymbol{\kappa}$ [10]. The corresponding principle of virtual work for a continuous couple-stress material occupying a volume $\mathcal{V}$ can then be written [10]

$$\int_{\mathcal{V}} \left(\boldsymbol{\sigma}^{(s)} : \delta\mathsf{E} - 2\boldsymbol{\mu}\cdot\delta\boldsymbol{\kappa}\right) \mathrm{d}V = \int_{\partial\mathcal{V}} (\boldsymbol{\tau}\cdot\delta\mathbf{u} + m\delta\omega)\,\mathrm{d}S. \tag{7}$$

Here $\boldsymbol{\tau} = \mathbf{n}\cdot\boldsymbol{\sigma}$ is a force traction at a surface with unit normal $\mathbf{n}$, and $m = \mathbf{n}\cdot\boldsymbol{\varepsilon}\boldsymbol{\mu}$ is a couple traction. We seek the discrete analogues of (1, 7) for a confluent monolayer of polygonal cells.

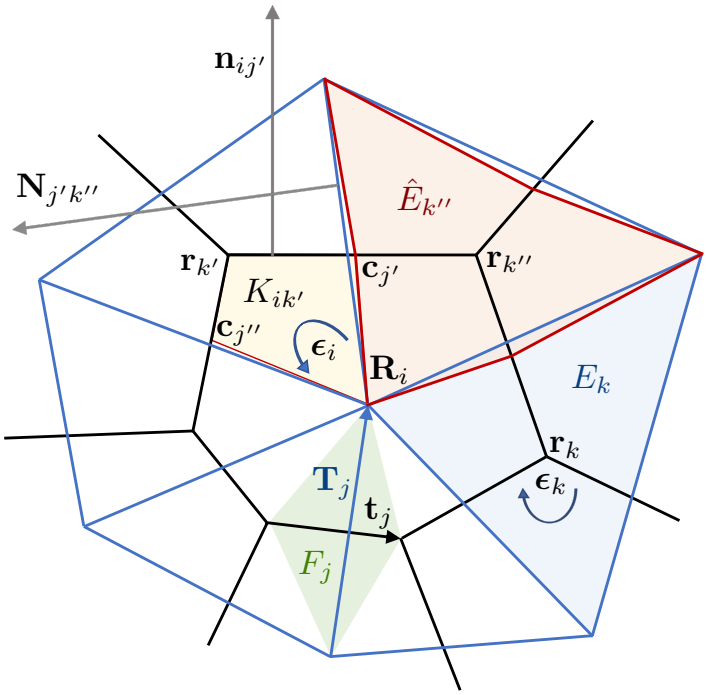

Figure 1: Sketch defining geometric objects, their orientations and their labels. Black lines denote cell edges, passing through vertices $\mathbf{r}_k$, $\mathbf{r}_{k'}$ and $\mathbf{r}_{k''}$; blue lines denote links between cell centres, including $\mathbf{R}_i$. Yellow: the kite of cell i at vertex k' with area $K_{ik'}$, with two of its vertices at edge centroids $\mathbf{c}_j$ and $\mathbf{c}_{j''}$. Green: the trapezium with area $\frac{1}{2}F_j$ [**fix figure**] spanned by edge $\mathbf{t}_j$ and link $\mathbf{T}_j$ (orientations of other edges and links are not shown). Blue: the triangle surrounding vertex k with area E_k. Orange: the tristar (made from three kites) surrounding vertex k'' with area $\hat{E}_{k''}$. Edge centroid $\mathbf{c}_{j'}$ sits on its boundary. Also shown are the outward normals $\mathbf{n}_{ij'}$ to cell i at edge j', and $\mathbf{N}_{j'k''}$, to triangle k'' at edge j'.

2.2 Geometrical preliminaries

Adopting notation used in [8], vertices, edges and faces of the (primal) cell network are labelled by k, j and i respectively. Orientations are assigned to each object and (signed) incidence matrices A_{jk} [B_{ij}] then define topological relationships between edges and vertices [faces and edges]. A and B also specify topological relationships between cell centres (assumed here to be cell vertex centroids), links between cell centres and triangular faces of the dual network. Vertices within the interior of a monolayer are assumed to neighbour three cells: vertex/face neighbours are identified by $\mathsf{C} = \frac{1}{2}\overline{\mathsf{B}}\,\overline{\mathsf{A}}$, where $\overline{\mathsf{A}}$ and $\overline{\mathsf{B}}$ are unsigned incidence matrices. We also identify centroids of each edge: each cell can then be partitioned into kites (labelled by ik) and a dual network can be constructed allowing the three kites neighbouring each vertex to form a 'tristar' with three vertices at cell centres (Figure 1). We also consider the dual triangulation defined by cell centroids. Neighbour exchanges are not considered in the present study, so that incidence matrices remain fixed.

The underlying space is the Euclidean plane with position vector $\mathbf{x}$. Where necessary, p, q, r denote subscripts of vectors and tensors identifying components with respect to a fixed basis in this plane. Orientations of faces $\boldsymbol{\epsilon}_i$ and $\boldsymbol{\epsilon}_k$ are prescribed as $\pm\boldsymbol{\varepsilon}$. $\boldsymbol{\epsilon}_i$ and $\boldsymbol{\epsilon}_k$ are taken to be independent of i and k respectively and of opposite sense. Orientations of edges $\mathbf{t}_j$ and links $\mathbf{T}_j$ are constrained such that

$$\mathbf{T}_j \cdot \boldsymbol{\epsilon}_i \mathbf{t}_j = \mathbf{t}_j \cdot \boldsymbol{\epsilon}_k \mathbf{T}_j = F_j > 0, \tag{8}$$

where $\frac{1}{2}F_j$ is the area of the trapezium spanned by t_j and T_j (Fig. 1).

On the primal network of cells, we define vertices by $\mathbf{r}_k$, edges by $\mathbf{t}_j = \sum_k A_{jk}\mathbf{r}_k$, edge lengths by $t_j = |\mathbf{t}_j|$ and edge centroids by $\mathbf{c}_j = \frac{1}{2}\sum_k \overline{A}_{jk}\mathbf{r}_k$. For cell i, the outward normal to edge j is $\mathbf{n}_{ij} = -\boldsymbol{\epsilon}_i B_{ij}\mathbf{t}_j$. The cell area

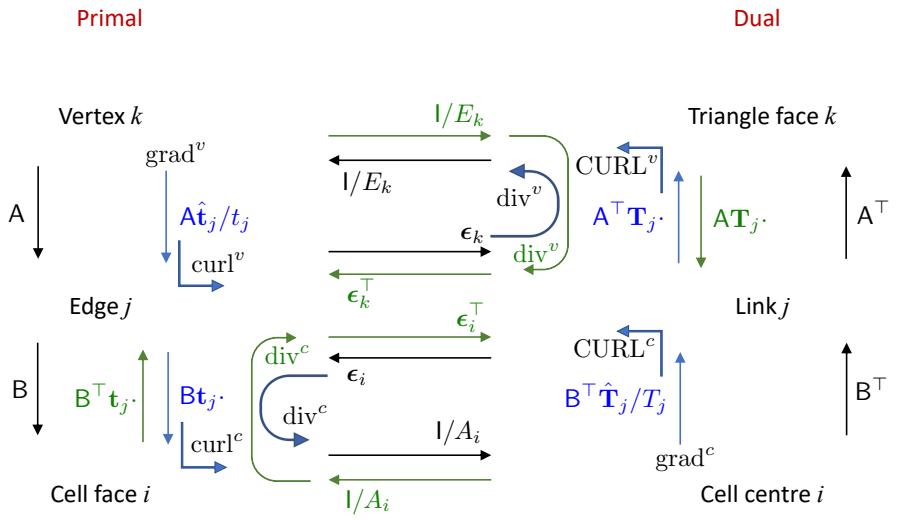

Figure 2: Topological operators A and B connect vertices, edges and faces of the primal (cell) network (left). A^T and B^T connect components of the dual network (a triangulation, right). Discrete differential operators (div, grad and two curls) defined on each network combine these with metric and orientational information. Divergence operators vary depending on whether they act on objects defined on edges/links or vertices/centres. The figure shows primary operators only, not derived operators, although only the eight operators shown need be considered when edges and links are orthogonal.

satisfies $\sum_j B_{ij}\mathbf{t}_j \otimes \mathbf{c}_j = A_i\boldsymbol{\epsilon}_i$, so that $A_i = \frac{1}{2}\sum_j \mathbf{n}_{ij}\cdot\mathbf{c}_j$, and the cell perimeter $L_i = \sum_j \overline{B}_{ij}t_j$. The number of edges of cell i is given by $Z_i = \sum_j \overline{B}_{ij}$. We define the centre of cell i as the vertex centroid $\mathbf{R}_i = Z_i^{-1}\sum C_{ik}\mathbf{r}_k$. Cell centres are vertices of the dual network (a triangulation). Links between cell centres are defined by $\mathbf{T}_j = \sum_i B_{ij}\mathbf{R}_i$. The outward normal to the triangle connecting adjacent cell centres is $\mathbf{N}_{jk} = -\boldsymbol{\epsilon}_k A_{jk}\mathbf{T}_j$ (Figure 1). We consider an isolated cellular monolayer occupying a simply connected domain. [*Discuss boundary conditions at the periphery.*]

[*Define E_k as triangle area, distinguish it from tristar area $\hat{E}_k$.*]

Appendix A describes how discrete analogues of grad, div and curl operators for scalars or tensors defined on vertices or cell centres, and vectors defined on edges or links, can be defined. Fig. 2 illustrates the four primary operators defined on each network, making eight in all. grad^v and grad^c act on scalars defined at vertices and cell centres (in vector spaces $\mathcal{V}$ and $\mathcal{C}$), creating vectors parallel to edges and links respectively. curl^v and CURL^c are similar but vectors are rotated to be normal to edges and links respectively. Vectors defined on edges on links sit in vector spaces $\mathcal{E}$ and $\mathcal{L}$. div^v and div^c measure fluxes of vectors normal to edges and links, returning a scalar at vertices and cell centres. CURL^v and curl^c act similarly, but measure fluxes parallel to edges and links. Explicit expressions for these operators are given in (40, 54).

When edges and links are non-orthogonal ($\mathbf{t}_j\cdot\mathbf{T}_j \neq 0$), as we assume to be the case, a further eight so-called derived operators (adjoints under a suitable inner product, denoted with a tilde) must be considered (see (56); definitions are given in (47) and (55)). Thereby we derive scalar Laplacians $\mathsf{L}_\mathcal{F} = -\mathrm{div}^c\circ\widetilde{\mathrm{grad}}^v = \mathrm{curl}^c\circ\widetilde{\mathrm{curl}}^c$ acting on cell faces, and $\mathsf{L}_\mathcal{V} = -\widetilde{\mathrm{div}}^c\circ\mathrm{grad}^v = \widetilde{\mathrm{curl}}^v\circ\mathrm{curl}^v$ on vertices, given by (49) and explicitly as

$$\{\mathsf{L}_\mathcal{F}\Psi^c\}_i = A_i^{-1}\textstyle\sum_{j,i'} B_{ij}\frac{t_j^2}{F_j}B_{i'j}\Psi_{i'}, \quad \{\mathsf{L}_\mathcal{V}\Psi^v\}_k = E_k^{-1}\textstyle\sum_{j,k'} A_{jk}\frac{F_j}{t_j^2}A_{jk'}\Psi_{k'}, \tag{9a}$$

for scalar functions defined on cell centres ($\{\Psi^c\}_i \equiv \Psi_i$) and vertices ($\{\Psi^v\}_k \equiv \Psi_k$) respectively. On the dual network, these have analogues $\mathsf{L}_\mathcal{C} = -\widetilde{\mathrm{div}}^v\circ\mathrm{grad}^c = \widetilde{\mathrm{CURL}}^c\circ\mathrm{CURL}^c$ acting on cell centres, $\mathsf{L}_\mathcal{T} =$

$-\mathrm{div}^v \circ \widetilde{\mathrm{grad}}^v = \mathrm{CURL}^v \circ \widetilde{\mathrm{CURL}}^v$ on triangles, where

$$\{\mathsf{L}_\mathcal{C}\Psi^c\}_i = A_i^{-1}\textstyle\sum_{j,i'} B_{ij}\dfrac{F_j}{T_j^2}B_{i'j}\Psi_{i'}, \quad \{\mathsf{L}_\mathcal{T}\Psi^v\}_k = E_k^{-1}\textstyle\sum_{j,k'} A_{jk}\dfrac{T_j^2}{F_j}A_{jk'}\Psi_{k'}. \tag{9b}$$

We can write $\mathsf{L}_\mathcal{T} \equiv \mathsf{E}^{-1}\mathsf{A}^\top\mathsf{T}_l\mathsf{A}$, where $\mathsf{E} = \mathrm{diag}(E_k)$ and $\mathsf{T}_l \equiv \mathrm{diag}(T_j^2/F_j)$. The matrices T_e and E^{-1} (which can be considered Hodge star operators) involve mappings from edges to links and faces to vertices respectively (Fig. 2) [*CHECK - expand explicity?*]. Likewise we can write $\mathsf{L}_\mathcal{F} \equiv \mathsf{H}^{-1}\mathsf{B}^\top\mathsf{T}_e\mathsf{B}$, where $\mathsf{H} = \mathrm{diag}(A_i)$ and $\mathsf{T}_e \equiv \mathrm{diag}(t_j^2/F_j)$. The four scalar Laplacians (9) reduce to two ($\mathsf{L}_\mathcal{T} = \mathsf{L}_\mathcal{V}$, $\mathsf{L}_\mathcal{F} = \mathsf{L}_\mathcal{C}$) in the special case of edge-link orthogonality, when $F_j = T_j t_j$.

[*Consider how operators change over tristars, rather than triangles.*]

A vector defined over edges or links can be represented in terms of potentials defined over each network, via a form of Helmholtz decomposition [11]. For any vector $\mathbf{h} \in \mathcal{E}$, its representation with regard to the primal network can be written [*explain proof*]

$$\mathbf{h} = \mathbf{h}^\parallel + \mathbf{h}^\perp \quad \text{where} \quad \mathbf{h}^\parallel = \mathrm{grad}^v\psi^v + \widetilde{\mathrm{curl}}^c\Psi^c \quad \text{and} \quad \mathbf{h}^\perp = -\widetilde{\mathrm{grad}}^v\psi^c + \mathrm{curl}^v\Psi^v, \tag{10}$$

for some ψ^v and $\Psi^v \in \mathcal{V}$, and for some ψ^c and $\Psi^c \in \mathcal{F}$, where $\mathbf{h}$ has been decomposed into its components parallel and perpendicular to each edge. Note that $\mathrm{curl}^v = \boldsymbol{\epsilon}_k\mathrm{grad}^v$ and $-\widetilde{\mathrm{grad}}^v = \boldsymbol{\epsilon}_k\widetilde{\mathrm{curl}}^c$. It follows that

$$\mathrm{div}^c\,\mathbf{h} = \mathrm{div}^c\,\mathbf{h}^\perp = -\mathrm{div}^c \circ \widetilde{\mathrm{grad}}^v\psi^c = \mathsf{L}_\mathcal{F}\psi^c, \quad \mathrm{curl}^c\,\mathbf{h} = \mathrm{curl}^c\,\mathbf{h}^\parallel = \mathrm{curl}^c \circ \widetilde{\mathrm{curl}}^c\,\Psi^c = \mathsf{L}_\mathcal{F}\Psi^c. \tag{11}$$

Note also that $\mathrm{div}^c \circ \mathrm{curl}^v\Psi^v = 0$.

The Helmholtz decomposition for a vector $\mathbf{h} \in \mathcal{L}$ follows a similar pattern. In this instance, we decompose $\mathbf{h}$ into components parallel and perpendicular to links:

$$\mathbf{h} = \mathbf{H}^\parallel + \mathbf{H}^\perp \quad \text{where} \quad \mathbf{H}^\parallel = \mathrm{grad}^c\hat{\psi}^c + \widetilde{\mathrm{CURL}}^v\hat{\Psi}^v \quad \text{and} \quad \mathbf{H}^\perp = -\widetilde{\mathrm{grad}}^c\hat{\psi}^v + \mathrm{CURL}^c\hat{\Psi}^c \tag{12}$$

for some $\hat{\psi}^c, \hat{\Psi}^c \in \mathcal{C}$ and $\hat{\psi}^v, \hat{\Psi}^v \in \mathcal{T}$. Note that $\mathrm{CURL}^c = \boldsymbol{\epsilon}_i\mathrm{grad}^c$ and $-\widetilde{\mathrm{grad}}^c = \boldsymbol{\epsilon}_i\widetilde{\mathrm{CURL}}^v$.Then

$$\mathrm{div}^v\,\mathbf{h} = \mathrm{div}^v\,\mathbf{H}^\perp = -\mathrm{div}^v \circ \widetilde{\mathrm{grad}}^c\hat{\psi}^v = \mathsf{L}_\mathcal{T}\hat{\psi}^v, \quad \mathrm{CURL}^v\,\mathbf{h} = \mathrm{CURL}^v\,\mathbf{H}^\perp = \mathrm{CURL}^v\,\widetilde{\mathrm{CURL}}^v\,\hat{\Psi}^v = \mathsf{L}_\mathcal{T}\hat{\Psi}^v. \tag{13a}$$

2.3 Force potential and microstress

A standard computational implementation of the vertex model yields forces $\mathbf{f}_{ik}$ that balance at each vertex and around each cell, so that (respectively)

$$\textstyle\sum_i C_{ik}\mathbf{f}_{ik} = \mathbf{0}, \quad \sum_k C_{ik}\mathbf{f}_{ik} = \mathbf{0}. \tag{14}$$

[*The former is enforced numerically; the latter is a consequence of the form of the microscopic stress (32), that ensures* $\mathrm{div}^c\tilde{\boldsymbol{\sigma}}_i^{(s)} = \mathbf{0}$.] These balances can be interpreted geometrically by rotating each force by $\pi/2$, so that forces form closed triangles around each vertex (14a) and closed loops around each cell (14b). The vertices of the network of rotated forces then define a force potential $\mathbf{h}_j$, via

$$\mathbf{f}_{ik} = -\textstyle\sum_j \boldsymbol{\epsilon}_i B_{ij}\mathbf{h}_j A_{jk}, \tag{15}$$

such that $\mathbf{h}_j - \mathbf{h}_{j'} = \sum -\boldsymbol{\varepsilon}\mathbf{f}_{ik}$, summing over a path connecting vertex j' to j [8]. The force stress for cell i can then be written as the first spatial moment of the forces acting on it [6], or equivalently in terms of force potential [8], as

$$A_i\boldsymbol{\sigma}_i = \textstyle\sum_k C_{ik}\mathbf{r}_k \otimes \mathbf{f}_{ik} = \sum_j B_{ij}(\mathbf{t}_j \otimes \mathbf{h}_j)\boldsymbol{\epsilon}_i, \quad E_k\boldsymbol{\sigma}_k = \sum_j A_{jk}(\mathbf{T}_j \otimes \mathbf{h}_j)\boldsymbol{\epsilon}_k, \tag{16}$$

where we have included the analogous force stress $\boldsymbol{\sigma}_k$ over triangles connecting cell centres.

Rather than integrate over a cell or triangle, we consider these stresses in microscopic form, using

$$A_i\tilde{\boldsymbol{\sigma}}_i = \cup_j B_{ij}(\mathbf{t}_j \otimes \mathbf{h}_j)\boldsymbol{\epsilon}_i, \quad E_k\tilde{\boldsymbol{\sigma}}_k = \cup_j A_{jk}(\mathbf{T}_j \otimes \mathbf{h}_j)\boldsymbol{\epsilon}_k. \tag{17}$$

Here B [A] attributes each edge [link] component to a neighbouring cell [triangle] face but maintains it as a distinct entity from the other edge [link] contributions. It follows immediately that $\mathbf{n}_{ij}\cdot\tilde{\boldsymbol{\sigma}}_i = 0$ for each edge j and $\mathbf{N}_{jk}\cdot\tilde{\boldsymbol{\sigma}}_k = 0$ for each link j, ensuring that $\mathrm{div}^c\,\tilde{\boldsymbol{\sigma}}_i = \mathbf{0}$ and $\mathrm{div}^v\,\tilde{\boldsymbol{\sigma}}_k = \mathbf{0}$.

We decompose $\mathbf{h}_j$ into components along $\mathbf{t}_j$ and $\boldsymbol{\epsilon_i}\mathbf{t}_j$, so that

$$\begin{aligned} A_i\tilde{\boldsymbol{\sigma}}_i &= \cup_j B_{ij}\left[\hat{\mathbf{t}}_j\otimes\hat{\mathbf{t}}_j(\mathbf{h}_j\cdot\mathbf{t}_j) + \hat{\mathbf{t}}_j\otimes(\boldsymbol{\epsilon}_i\hat{\mathbf{t}}_j)(\mathbf{h}_j\cdot(\boldsymbol{\epsilon}_i\mathbf{t}_j))\right]\boldsymbol{\epsilon}_i \\ &= \cup_j B_{ij}\left[\hat{\mathbf{t}}_j\otimes\hat{\mathbf{n}}_{ij}(\mathbf{h}_j\cdot\mathbf{t}_j) + \hat{\mathbf{t}}_j\otimes\hat{\mathbf{t}}_j(\mathbf{h}_j\cdot(\boldsymbol{\epsilon}_i\mathbf{t}_j))\right]. \end{aligned} \tag{18}$$

Then $A_i\mathrm{Tr}(\tilde{\boldsymbol{\sigma}}_i) = \sum_{j'} B_{ij'}\mathbf{h}_{j'}\cdot(\boldsymbol{\epsilon}_i\mathbf{t}_{j'})$ so that the deviatoric stress becomes

$$A_i\tilde{\boldsymbol{\sigma}}_i^D = \cup_j B_{ij}\left[\hat{\mathbf{t}}_j\otimes\hat{\mathbf{n}}_{ij}(\mathbf{h}_j\cdot\mathbf{t}_j) + \hat{\mathbf{t}}_j\otimes\hat{\mathbf{t}}_j(\mathbf{h}_j\cdot(\boldsymbol{\epsilon}_i\mathbf{t}_j))\right] - \tfrac{1}{2}\mathsf{I}\textstyle\sum_{j'} B_{ij'}\mathbf{h}_{j'}\cdot(\boldsymbol{\epsilon}_i\mathbf{t}_{j'}). \tag{19}$$

The final term involves $\sum_j$ rather than $\cup_j$, ensuring that $\mathrm{div}^c\,\tilde{\boldsymbol{\sigma}}_i^D = \mathbf{0}$. $\tilde{\boldsymbol{\sigma}}_i^D$ has symmetric component

$$A_i\check{\tilde{\boldsymbol{\sigma}}}_i^D = \cup_j B_{ij}\left[\tfrac{1}{2}(\hat{\mathbf{t}}_j\otimes\hat{\mathbf{n}}_{ij} + \hat{\mathbf{n}}_{ij}\otimes\hat{\mathbf{t}}_j)(\mathbf{h}_j\cdot\mathbf{t}_j) + \hat{\mathbf{t}}_j\otimes\hat{\mathbf{t}}_j(\mathbf{h}_j\cdot(\boldsymbol{\epsilon}_i\mathbf{t}_j))\right] - \tfrac{1}{2}\mathsf{I}\textstyle\sum_{j'} B_{ij'}\mathbf{h}_{j'}\cdot(\boldsymbol{\epsilon}_i\mathbf{t}_{j'}) \tag{20}$$

and antisymmetric component

$$A_i\tilde{\boldsymbol{\sigma}}_i^{(a)} = \cup_j B_{ij}\tfrac{1}{2}(\hat{\mathbf{t}}_j\otimes\hat{\mathbf{n}}_{ij} - \hat{\mathbf{n}}_{ij}\otimes\hat{\mathbf{t}}_j)(\mathbf{h}_j\cdot\mathbf{t}_j) = \tfrac{1}{2}\boldsymbol{\epsilon}_i\cup_j B_{ij}(\mathbf{h}_j\cdot\mathbf{t}_j), \tag{21}$$

where we have used $\hat{\mathbf{t}}_j\otimes\hat{\mathbf{n}}_{ij} - \hat{\mathbf{n}}_{ij}\otimes\hat{\mathbf{t}}_j \equiv \boldsymbol{\epsilon}_i$ (consider its action on a vector $\alpha\hat{\mathbf{t}_j} + \beta\hat{\mathbf{n}}_{ij}$). These relations demonstrate how, by writing the microscale stress in terms of a force potential $\mathbf{h}_j$, the stress is automatically divergence-free. We can interpret $\mathbf{h}_j\cdot\mathbf{t}_j$ in (21) as a torque exerted on each edge of the cell. Analogous expressions to (18-21) follow immediately for $\tilde{\boldsymbol{\sigma}}_k$, after projecting $\mathbf{h}_j$ onto $\mathbf{T}_j$ and $\boldsymbol{\epsilon}_k\mathbf{T}_j$.

The cell and tristar force-stresses can be recovered from microstresses by replacing $\cup_j$ with $\sum_j$ in (17), as in [8], to give (16). It follows that

$$P_{\mathrm{eff}i} \equiv \tfrac{1}{2}\mathrm{Tr}(\boldsymbol{\sigma}_i) = -\tfrac{1}{2}\{\mathrm{div}^c\,\mathbf{h}\}_i, \qquad \boldsymbol{\sigma}_i^{(a)} = \tfrac{1}{2}\boldsymbol{\epsilon}_i\{\mathrm{curl}^c\,\mathbf{h}\}_i, \tag{22a}$$

$$P_{\mathrm{eff}k} \equiv \tfrac{1}{2}\mathrm{Tr}(\boldsymbol{\sigma}_k) = -\tfrac{1}{2}\{\mathrm{div}^v\,\mathbf{h}\}_k, \qquad \boldsymbol{\sigma}_k^{(a)} = \tfrac{1}{2}\boldsymbol{\epsilon}_k\{\mathrm{CURL}^v\,\mathbf{h}\}_k. \tag{22b}$$

With $\mathbf{t}_j\cdot\mathbf{T}_j \neq 0$ in general, we see how the projections of $\mathbf{h}_j$ onto edges and links (in curls) play a distinct role from the projections on normals to cells and tristars (in divergences). (For the time being we forego imposing the requirement for $\boldsymbol{\sigma}_i$ to be symmetric, i.e. that $\sum_j B_{ij}\mathbf{h}_j\cdot\mathbf{t}_j = 0$.)

[*The stresses over a chain* $\mathbf{d}$ *of neighbouring cells is equivalent to the loading around its periphery* $\mathsf{B}^\top\mathbf{d}$*, because* $\sum_i d_i A_i\boldsymbol{\sigma}_i = \sum_{i,j} d_i B_{ij}\mathbf{t}_j\otimes\mathbf{h}_j\boldsymbol{\epsilon}_i$.]

2.4 Discrete stress potentials

We now pursue the discrete analogue of (1), The force potential can be expressed in terms of scalar potentials using (10) and (12), so that

$$\mathrm{Tr}(\boldsymbol{\sigma}_i) = -\{\mathsf{L}_{\mathcal{F}}\psi^c\}_i, \qquad \boldsymbol{\sigma}_i^{(a)} = \tfrac{1}{2}\boldsymbol{\epsilon}_i\{\mathsf{L}_{\mathcal{T}}\Psi^c\}_i, \tag{23a}$$

$$\mathrm{Tr}(\boldsymbol{\sigma}_k) = -\{\mathsf{L}_{\mathcal{T}}\hat{\psi}^v\}_k, \qquad \boldsymbol{\sigma}_k^{(a)} = \tfrac{1}{2}\boldsymbol{\epsilon}_k\{\mathsf{L}_{\mathcal{T}}\hat{\Psi}^v\}_k. \tag{23b}$$

We construct vectors orthogonal to $\mathbf{h}$

$$-\boldsymbol{\epsilon}_i\mathbf{h} = (\mathrm{curl}^v\psi^v - \widetilde{\mathrm{grad}}^v\,\Psi^c) - (\widetilde{\mathrm{curl}}^c\,\psi^c + \mathrm{grad}^v\Psi^v), \tag{24a}$$

$$-\boldsymbol{\epsilon}_k\mathbf{h} = (\mathrm{CURL}^c\hat{\psi}^c - \widetilde{\mathrm{grad}}^c\,\hat{\Psi}^v) - (\widetilde{\mathrm{CURL}}^v\,\hat{\psi}^v + \mathrm{grad}^c\hat{\Psi}^c), \tag{24b}$$

and then, by analogy with (5), we consider

$$\mathsf{S}^c = \mathrm{curl}^c \otimes (-\boldsymbol{\epsilon}_i \mathbf{h}^c) \quad \text{and} \quad \mathsf{S}^v = \mathrm{CURL}^v \otimes (-\boldsymbol{\epsilon}_k \mathbf{h}^v) \tag{25}$$

as potential representations of $\boldsymbol{\sigma}_i$ and $\boldsymbol{\sigma}_k$ respectively. Contracting, $\mathrm{Tr}(\mathsf{S}^c) = \mathrm{curl}^c \circ (-\mathbf{g}^c) = -\mathsf{L}_{\mathcal{F}}\psi^c$ ($\mathrm{curl}^c \otimes \mathrm{curl}^v = 0$ because of geometry and $\mathrm{curl}^c \otimes \mathrm{grad}^v = 0$ because of topology). Likewise $\mathrm{Tr}(\mathsf{S}^v) = \mathrm{CURL}^v \circ (-\mathbf{g}^v) = -\mathsf{L}_{\mathcal{T}}\hat{\psi}^v$. From (54),

$$(\mathrm{CURL}^v \otimes \widetilde{\mathrm{grad}}^c \hat{\Psi}^v)_{k,pq} = \frac{1}{E_k} \sum\nolimits_{j,k'} \frac{\{\mathbf{T}_j \otimes (\boldsymbol{\epsilon}_k \mathbf{T}_j)\}_{pq}}{F_{j'}} A_{jk'} \hat{\Psi}^v_{k'}. \tag{26}$$

Using [CHECK]

$$\tfrac{1}{2}(\{\mathbf{T}_j \otimes (\boldsymbol{\epsilon}_k \mathbf{T}_j)\}_{pq} - \{\mathbf{T}_j \otimes (\boldsymbol{\epsilon}_k \mathbf{T}_j)\}_{qp}) = -\tfrac{1}{2}\boldsymbol{\epsilon}_k T_j^2 \tag{27}$$

we see that $(\mathrm{CURL}^v \otimes \widetilde{\mathrm{grad}}^c \hat{\Psi}^v)^{(a)}_k = -\frac{1}{2}\boldsymbol{\epsilon}_k \mathsf{L}_{\mathcal{T}} \hat{\Psi}^v$, and therefore $\mathsf{S}^{v(a)} = \frac{1}{2}\boldsymbol{\epsilon}_k \mathsf{L}_{\mathcal{T}} \hat{\Psi}^v$. Likewise $\mathsf{S}^{c(a)} = \frac{1}{2}\boldsymbol{\epsilon}_k \mathsf{L}_{\mathcal{F}} \Psi^c$ [*Show that remaining antisymmetric components vanish.*]. The conditions in (23) are therefore satisfied.

2.5 Virtual work - derivation

3 Introducing a constitutive model

3.1 Virtual work in the vertex model

We introduce an energy per cell $U_i = U(A_i, L_i)$ and define a pressure and tension as $\mathcal{P}_i \equiv \partial U/\partial A_i$ and $\mathcal{T}_i \equiv \partial U/\partial L_i$ respectively. The total energy of the monolayer is $\mathcal{U} = \sum_i U_i$. This is a function of vertex locations, via the dependence of areas and perimeters on $\mathbf{r}_k$. Suppose the monolayer is in a stationary equilibrium configuration (denoted with a prime) and consider virtual displacements $\delta\mathbf{r}_k$ of its vertices. The expansion

$$\mathcal{U} = \mathcal{U}' + \sum\nolimits_{i,k} \left(\frac{\partial U_i}{\partial \mathbf{r}_k}\right)' \cdot \delta\mathbf{r}_k + \sum\nolimits_{i,k,k'} \delta\mathbf{r}_k \cdot \left(\frac{\partial^2 U_i}{\partial \mathbf{r}_k \partial \mathbf{r}_{k'}}\right)' \cdot \delta\mathbf{r}_k + \dots \tag{28}$$

reveals the force $\mathbf{f}_{ik} \equiv \partial U_i/\partial \mathbf{r}_k$ exerted at vertex k by cell i. The sum of all forces at each vertex vanishes when the monolayer is at an equilibrium, i.e. $\sum_i C_{ik}\mathbf{f}_{ik} = \mathbf{0}$ for all k. The second variation in (28) captures weakly nonlinear effects and establishes the stability or otherwise of the equilibrium. We work below with the first variation, but consider how the forces organise into stresses acting over cells.

It is sufficient for our purposes to restrict attention to variations that can be expressed as a smooth function of position under a deformation $\mathbf{u}(\mathbf{x})$, i.e. we map vertices from $\mathbf{r}'_k$ to $\mathbf{r}_k = \mathbf{r}'_k + \mathbf{u}(\mathbf{r}'_k)$ so that $\delta\mathbf{r}_k = \mathbf{u}(\mathbf{r}'_k)$. In the following, we will neglect effects that are quadratic in $\mathbf{u}$ but account for first- and second-order deformation gradients $\nabla\mathbf{u}$ and M. We will then reformulate the first variation in (28) in terms of E, $\nabla\mathsf{E}$ and $\boldsymbol{\kappa}$, to determine the conjugate stresses. We will gather terms over cells, and also repartition them over the dual triangulation, to identify stresses over cells and tristars. In doing so, we interpolate deformation gradients evaluated on vertices onto edge centroids and cell centres, using Taylor expansion to capture the leading-order effect of spatial variations. Accordingly, we use subscripts i, j and k to describe fields evaluated at cell centres, edge centroids and vertices, writing $\mathbf{u}_i \equiv \mathbf{u}(\mathbf{R}'_i)$, $\mathbf{u}_j \equiv \mathbf{u}(\mathbf{c}'_j)$ and $\mathbf{u}_k = \mathbf{u}(\mathbf{r}'_k)$ and so on.

We retain second derivatives of $\mathbf{u}$ but discard third and higher derivatives, assuming deformations vary over scales long compared to the size of individual cells. As shown in Appendix B, the changes in cell perimeter and area to this order are

$$L_i = L'_i\left[1 + \mathsf{Q}_i : \mathsf{E}_i + \mathsf{X}_i \vdots (\nabla\mathsf{E})_i\right], \tag{29a}$$

$$A_i = A'_i\left[1 + \mathsf{I} : \mathsf{E}_i + \mathsf{Y}_i \vdots (\nabla\mathsf{E})_i + \left[\frac{1}{8A'_i}\sum\nolimits_j (t'_j)^2 \mathbf{n}'_{ij}\right] \cdot \boldsymbol{\kappa}_i\right], \tag{29b}$$

where $L'_i\mathsf{Q}_i \equiv \sum_j \overline{B}_{ij}\mathbf{t}'_j \otimes \hat{\mathbf{t}}'_j$. The third-order tensors X_i and Y_i (see (63, 68)) characterise the impact of strain gradients on cell perimeter and area respectively. They are size-dependent, as is appropriate for objects that

measure a gradient. W does not change perimeter to this order, but it alters cell area through the curvature $\boldsymbol{\kappa}$.

Returning to (28), the energy maps from $\mathcal{U}_0 \equiv \mathcal{U}'$ [*include boundary forcing?*] to

$$\begin{aligned}\mathcal{U} = \textstyle\sum_i U_i(A_i, L_i) &= U' + \textstyle\sum_i [\mathcal{P}_i'(A_i - A_i') + \mathcal{T}_i'(L_i - L_i')] + \dots \\ &= U' + \textstyle\sum_i \left\{ A_i' \boldsymbol{\sigma}_i^{(s)} : \mathsf{E}_i + (\mathcal{P}_i A_i' \mathsf{Y}_i + \mathcal{T}_i L_i' \mathsf{X}_i) \vdots \nabla \mathsf{E}_i - 2A_i' \boldsymbol{\mu}_i \cdot \boldsymbol{\kappa}_i \right\} + \dots, \end{aligned} \tag{30}$$

using (29) and neglecting quantities that are quadratic in strains. Comparison with (7) reveals the leading-order symmetric force-stress tensor and couple stress vector of cell i as

$$\boldsymbol{\sigma}_i^{(s)} = \mathcal{P}_i' \mathsf{I} + \frac{\mathcal{T}_i' L_i'}{A_i'} \mathsf{Q}_i, \quad \boldsymbol{\mu}_i = -\frac{\mathcal{P}_i'}{16 A_i'} \textstyle\sum_j (t_j')^2 \mathbf{n}_{ij}'. \tag{31}$$

The isotropic stress has magnitude $P_{\text{eff},i} = \mathcal{P}_i' + \frac{1}{2}\mathcal{T}_i' L_i'/A_i'$. Given that $\sum_j \mathbf{n}_{ij}' = \mathbf{0}$, the couple stress vector vanishes for symmetric cells, for which t_j' is uniform.

[*Notational point: distinguish stress derived from virtual work from stress derived as first moment of force*]

It is important to draw a distinction between $\boldsymbol{\sigma}_i^{(s)}$ in (31), the force stress integrated over cell i, and the corresponding *microscopic* cell stress

$$\tilde{\boldsymbol{\sigma}}_i^{(s)} = \mathcal{P}_i' \mathsf{I} + \frac{\mathcal{T}_i'}{A_i'} \cup_j \overline{B}_{ij} \mathbf{t}_j' \otimes \hat{\mathbf{t}}_j', \tag{32}$$

which retains edge-to-edge variation rather than averaging over the perimenter. This stress has zero divergence, because evaluating $\text{div}^c \tilde{\boldsymbol{\sigma}}_i^{(s)}$ using (57) includes $\sum_j \mathbf{n}_{ij}'$ summed around a closed loop, which vanishes, and $\sum_j \mathbf{n}_{ij}' \cdot \mathbf{t}_j' \otimes \hat{\mathbf{t}}_j'$, which also vanishes as $\mathbf{n}_{ij}' \cdot \mathbf{t}_j' = 0$ along each edge. This ensures zero net force on each cell [*verify*]. In general, however, $\mathbf{n}_{ij} \cdot \mathsf{Q}_i \neq \mathbf{0}$ and so $\text{div}^c \boldsymbol{\sigma}_i^{(s)}$ does not vanish.

Repartitioning the first variation of energy over kites allows the stress over tristars to be expressed explicilty, as shown in Appendix C. For later reference, it is also helpful to repartition the contribution to the energy associated with couple stress vector. As gradients in curvature across the monolayer will not play a role in what follows, we take $\boldsymbol{\kappa}$ to be uniform, and drop primes, to define the couple-stress vector attributed to edges as

$$\textstyle\sum_i A_i(-2\boldsymbol{\mu}_i \cdot \boldsymbol{\kappa}) = \sum_j F_j(-2\boldsymbol{\mu}_j \cdot \boldsymbol{\kappa}) \quad \text{where} \quad \boldsymbol{\mu}_j = -\frac{t_j^2}{16 F_j} \textstyle\sum_i \mathcal{P}_i \mathbf{n}_{ij}, \tag{33}$$

where area is partitioned into trapezia of area F_j, associated with edge/link j. $\boldsymbol{\mu}_j$ has zero curl around cells (because it acts along normals to edges), but has non-zero curl around triangles of the dual network:

$$\mathcal{C}_k \equiv \{\text{curl}^v \boldsymbol{\mu}\}_k = E_k^{-1} \textstyle\sum_j A_{jk} \mathbf{T}_j \cdot \boldsymbol{\mu}_j = \frac{1}{16 E_k} \sum_{i,j} \mathcal{P}_i B_{ij} t_j^2 A_{jk}. \tag{34}$$

As we show below, this can be related to the torque experienced in the neighbourhood of cellular trijunction k. The pressure difference across edge j, $\sum_i B_{ij}\mathcal{P}_i$, is multiplied by t_j^2 to give a moment, and the three contributions to the moment at the trijunction are summed at the vertex. $\mathcal{C}_k$ vanishes if pressures are uniform ($\sum_i \mathcal{P}_i B_{ij} = 0$) or if the edges are of uniform size (because $\mathsf{BA} = \mathsf{0}$).

The couple traction on a surface of the cell with normal $\mathbf{n}$ *is* $m = \mathbf{n} \cdot \boldsymbol{\varepsilon}\boldsymbol{\mu}$*, implying that the cell experiences a bending moment that is symmetric about* $\boldsymbol{\varepsilon}\boldsymbol{\mu}$*. Note that* $\sum_j \mathbf{n}_{ij}' = \mathbf{0}$*; the* t_j^2 *weighting favours longer walls.*

3.2 Potentials for the vertex model

We now return to the representation of force potential using scalar potentials (10) and (12). To ensure zero couple on cells, we take $\Psi^c = 0$. Then $\text{curl}^c \mathbf{h}$ vanishes (so that $\boldsymbol{\sigma}_i^{(a)} = \mathsf{0}$ in (22)) but $\text{CURL}^v \mathbf{h} = \mathsf{L}_{\mathcal{T}} \hat{\Psi}^v$ is

non-zero (giving non-zero torque on triangles). We identify the couple stress vector as $\boldsymbol{\mu} = -\mathrm{curl}^v \Psi^v$, which is normal to edges, satisfying $\mathrm{div}^c \boldsymbol{\mu} = \mathbf{0}$. In general we expect $\boldsymbol{\mu}$ to be described by non-zero $\hat{\Psi}^v$ and $\hat{\Psi}^c$.

The torque on a tristar is given by the antisymmetric component of the Cauchy stress, multiplied by the cell or tristar area. [*Check triangle vs tristar!*]. However, a further condition must be satisfied: equating $\{\mathrm{curl}^v \boldsymbol{\Psi}^v\}_k = \sum_k A_{jk} \Psi_k \boldsymbol{\epsilon}_k \mathbf{t}_j / t_j^2$ with $\boldsymbol{\mu}_j$ in (33) gives $\sum_k A_{jk} \Psi_k = \sum_{i'} \mathcal{P}_{i'} B_{i'j} (t_j^4/(16 F_j))$. Summing over a cell, by applying $\sum_j B_{ij}$, imposes the following constraint, equivalent to requiring that $\mathrm{div}^c \boldsymbol{\mu} = 0$:

$$0 = \sum_{i',j} B_{ij} \frac{t_j^4}{F_j} B_{i'j} \mathcal{P}_{i'}. \tag{35}$$

This implies that $\mathcal{P}$ lies in the nullspace of $\mathsf{BCB}^\top$ where $\mathsf{C} \equiv \mathrm{diag}(t_j^4/F_j)$. This is a necessary condition for the existence of the Mindlin stress function, and for torque balance to be satisfied while accounting for couple stress.

A strategy for determining potentials is as follows.

1. On the primal network, solve $\mathsf{L}_\mathcal{F} \psi^c = \mathrm{div}^c \mathbf{h}$ (subject to suitable boundary conditions) to determine ψ^c.
2. With $\Psi^c = 0$, determine ψ^v as a line integral of $\mathbf{h}^\parallel$ (or use $\mathsf{L}_\mathcal{V} \psi^v = -\widetilde{\mathrm{div}}^c \mathbf{h}$).
3. With $\mathrm{div}^c \boldsymbol{\mu} = 0$, determine Ψ^v as a line integral of $\boldsymbol{\mu}$ (or use $\mathsf{L}_\mathcal{V} \Psi^v = \widetilde{\mathrm{curl}}^v \mathbf{h}$).
4. On the dual network, solve $\mathsf{L}_\mathcal{F} \hat{\psi}^v = \mathrm{div}^v \mathbf{h}$ (subject to suitable boundary conditions) to determine $\hat{\psi}^v$.
5. Solve $\mathsf{L}_\mathcal{T} \hat{\Psi}^v = \mathrm{CURL}^v \mathbf{h}$ to determine $\hat{\Psi}^v$.
6. Use $\mathsf{L}_\mathcal{C} \hat{\psi}^c = -\widetilde{\mathrm{div}}^v \mathbf{h}$ to determine $\hat{\psi}^c$.
7. Use $\mathsf{L}_\mathcal{C} \hat{\Psi}^c = \widetilde{\mathrm{CURL}}^c \mathbf{h}$ to determine $\hat{\Psi}^c$.

The potentials on the dual network depend on the choice of cell centres, because the forcing terms in steps 4 to 7 depend on the definition of links. However that when edges and links are orthogonal, $\mathsf{L}_\mathcal{C} = \mathsf{L}_\mathcal{F}$ and $\mathrm{div}^c = -\widetilde{\mathrm{div}}^v$, so that steps 1 and 6 are identical and $\hat{\psi}^c = \psi^c$; $\mathsf{L}_\mathcal{V} = \mathsf{L}_\mathcal{T}$ and $\mathrm{div}^v = -\widetilde{\mathrm{div}}^c$ so that steps 2 and 4 are identical and $\hat{\psi}^v = \psi^v$; $\mathrm{CURL}^v = \widetilde{\mathrm{curl}}^v$ so that steps 3 and 5 are identical and $\hat{\Psi}^v = \Psi^v$; and $\widetilde{\mathrm{CURL}}^c = \mathrm{curl}^c$ so that $\hat{\Psi}^c = 0$ in step 7. (Where a potential is uniformly constant, we take it to be zero without loss of generality.)

[*Uniqueness and solubility of the Laplacian problems needs to be established.*]

Relate potentials defined over kites to scalars ψ^c, ψ^v:

$$\mathbf{h}_j = \{\mathrm{CURL}^c \boldsymbol{\Psi}^c\}_j + \{\mathrm{curl}^v \boldsymbol{\Psi}^v\}_j + \{\mathrm{grad}^c \boldsymbol{\psi}^c\}_j + \{\mathrm{grad}^v \boldsymbol{\psi}^v\}_j \tag{36}$$

$$\equiv \frac{\boldsymbol{\epsilon}_k \mathbf{T}_j}{T_j^2} \sum_i B_{ij} \Psi_i + \frac{\boldsymbol{\epsilon}_i \mathbf{t}_j}{t_j^2} \sum_k A_{jk} \Psi_k + \frac{\mathbf{T}_j}{T_j^2} \sum_i \overline{A}_{jk} B_{ij} \psi_{ik} + \frac{\mathbf{t}_j}{t_j^2} \sum_k A_{jk} \overline{B}_{ij} \psi_{ik} \tag{37}$$

4 Discussion

Helmholtz decomposition of the rotated force potential identifies two scalar potentials, identifiable as Airy and Mindlin stress functions. In general, seven potentials can be identified using four Laplacians.

The curl of a scalar field (the Mindlin stress function) defined on vertices defines a couple stress vector defined on links; a further curl defines the torque on vertices as a vertex Laplacian of the stress function.

The theory is linear and weakly nonlocal.

Couple stress is experienced in the neighbourhood of each trijunction, even though there is no net torque on each cell.

Viscous effects: consider time-derivatives of area and pressure.

Explain microstress versus averaged stress.

[8]: orthocentric condition for stresses to be defined in terms of a common potential?

A Discrete operators in 2D

The discrete analogues of differential operators appear in a variety of forms, being defined over primal and dual networks and acting on variables defined on vertices, edges, and faces of each [12]. These are summarised in Fig. 2, which shows the primary operators on the cell network (grad^v, curl^v, curl^c and div^c) and on the dual network (grad^c, CURL^v, CURL^c and div^v).

A.1 Operators on the primary network

We define vector spaces $\mathcal{V}$, $\mathcal{E}$, $\mathcal{F}$ of fields defined on vertices, edges and faces, with associated inner products $[\cdot,\cdot]_\mathcal{V}$, $[\cdot,\cdot]_\mathcal{E}$, $[\cdot,\cdot]_\mathcal{F}$, represented by matrices $\mathsf{M}^\mathcal{V}$, $\mathsf{M}^\mathcal{E}$, $\mathsf{M}^\mathcal{F}$. Thus

$$[\phi,\psi]_\mathcal{V} \equiv \textstyle\sum_{k,k'}\phi_k M^\mathcal{V}_{kk'}\psi_{k'}, \quad [\mathbf{u},\mathbf{v}]_\mathcal{E} \equiv \textstyle\sum_{j,j'}\mathbf{u}_j^\top \mathsf{M}^\mathcal{E}_{jj'}\mathbf{v}_{j'}, \quad [f,g]_\mathcal{F} \equiv \textstyle\sum_{i,i'} f_i M^\mathcal{F}_{ii'} g_{i'} \tag{38}$$

for any $\phi,\psi\in\mathcal{V}$, $\mathbf{u},\mathbf{v}\in\mathcal{E}$, $f,g\in\mathcal{F}$ (typically, we consider vectors defined on edges and scalars on vertices and faces). We reserve bold font for vectors in $\mathbb{R}^2$. Below we will assume that

$$\mathsf{M}^\mathcal{V} = \mathrm{diag}(E_k), \quad \mathsf{M}^\mathcal{E} = \mathrm{diag}(\mathsf{I}F_j), \quad \mathsf{M}^\mathcal{F} = \mathrm{diag}(A_i). \tag{39}$$

$\mathsf{M}^\mathcal{E}$ is chosen to have dimensions of area and to be symmetric between edges and links. I in (39) is the 2×2 identity.

The 'primary operators' over cells are $\mathrm{grad}^v : \mathcal{V}\to\mathcal{E}$, $\mathrm{curl}^v : \mathcal{V}\to\mathcal{E}$, $\mathrm{curl}^c : \mathcal{E}\to\mathcal{F}$ and $\mathrm{div}^c : \mathcal{E}\to\mathcal{F}$, and are defined by

$$\{\mathrm{grad}^v\,\phi\}_j = \textstyle\sum_k A_{jk}\dfrac{\mathbf{t}_j}{t_j^2}\phi_k, \qquad \{\mathrm{curl}^c\,\mathbf{b}\}_i = \dfrac{1}{A_i}\textstyle\sum_j B_{ij}\mathbf{t}_j\cdot\mathbf{b}_j, \tag{40a}$$

$$\{\mathrm{curl}^v\phi\}_j = \textstyle\sum_k \dfrac{\boldsymbol{\epsilon}_k\mathbf{t}_j}{t_j^2}A_{jk}\phi_k, \qquad \{\mathrm{div}^c\,\mathbf{b}\}_i = -\dfrac{1}{A_i}\textstyle\sum_j B_{ij}(\boldsymbol{\epsilon}_i\mathbf{t}_j)\cdot\mathbf{b}_j, \tag{40b}$$

We can write these in matrix form as

$$\mathrm{grad}^v = (\mathsf{N}^\mathcal{E})^{-1}\mathsf{A}\mathsf{N}^\mathcal{V}, \qquad \mathrm{curl}^c = (\mathsf{N}^\mathcal{F})^{-1}\mathsf{B}\mathsf{N}^\mathcal{E}, \tag{41a}$$

$$\mathrm{curl}^v = (\tilde{\mathsf{N}}^\mathcal{E})^{-1}\mathsf{A}\mathsf{N}^\mathcal{V}, \qquad \mathrm{div}^c = (\mathsf{N}^\mathcal{F})^{-1}\mathsf{B}\tilde{\mathsf{N}}^\mathcal{E}. \tag{41b}$$

where $\mathsf{N}^\mathcal{V}=\mathsf{I}$, $\mathsf{N}^\mathcal{E}=\mathrm{diag}(\mathbf{t}_j^\top)$, $\mathsf{N}^\mathcal{F}=\mathrm{diag}(A_i)$ and $\tilde{\mathsf{N}}^\mathcal{E}=\mathrm{diag}(-(\boldsymbol{\epsilon}_i\mathbf{t}_j)^\top)$ (so $(\mathsf{N}^\mathcal{E})^{-1}=\mathrm{diag}(\mathbf{t}_j/t_j^2)$, $(\tilde{\mathsf{N}}^\mathcal{E})^{-1}=\mathrm{diag}((\boldsymbol{\epsilon}_k\mathbf{t}_j)/t_j^2)$). The topological relationship $\mathsf{BA}=\mathsf{0}$ ensures that $\mathrm{curl}^c\circ\mathrm{grad}^v=0$ and $\mathrm{div}^c\circ\mathrm{curl}^v=0$. These exact sequences (de Rahm complexes) can be represented using the commutative diagrams

$$\begin{array}{ccccc}
\mathcal{V} & \xrightarrow{\mathrm{grad}^v} & \mathcal{E} & \xrightarrow{\mathrm{curl}^c} & \mathcal{F} \\
\downarrow{\scriptstyle \mathsf{N}^\mathcal{V}} & & \downarrow{\scriptstyle \mathsf{N}^\mathcal{E}} & & \downarrow{\scriptstyle \mathsf{N}^\mathcal{F}} \\
\mathcal{V} & \xrightarrow{\mathsf{A}} & \mathcal{E} & \xrightarrow{\mathsf{B}} & \mathcal{F}
\end{array}
\quad\text{and}\quad
\begin{array}{ccccc}
\mathcal{V} & \xrightarrow{\mathrm{curl}^v} & \mathcal{E} & \xrightarrow{\mathrm{div}^c} & \mathcal{F} \\
\downarrow{\scriptstyle \mathsf{N}^\mathcal{V}} & & \downarrow{\scriptstyle \tilde{\mathsf{N}}^\mathcal{E}} & & \downarrow{\scriptstyle \mathsf{N}^\mathcal{F}} \\
\mathcal{V} & \xrightarrow{\mathsf{A}} & \mathcal{E} & \xrightarrow{\mathsf{B}} & \mathcal{F}
\end{array}
\quad . \tag{42}$$

The left-hand sequence generates vectors oriented tangentially to edges; the right-hand sequence generates vectors oriented normally to edges. [*Check for transposes in curls.*]

Adjoints of the primary operators (denoted with $*$) under inner products (38) satisfy

$$[\mathrm{grad}^v\,\phi,\mathbf{b}]_\mathcal{E} = [\phi,\mathrm{grad}^{v*}\,\mathbf{b}]_\mathcal{V}, \qquad [\mathrm{curl}^c\,\mathbf{b},f]_\mathcal{F} = [\mathbf{b},\mathrm{curl}^{c*}f]_\mathcal{E}, \tag{43a}$$

$$[\mathrm{curl}^v\,\phi,\mathbf{b}]_\mathcal{E} = [\phi,\mathrm{curl}^{v*}\,\mathbf{b}]_\mathcal{V}, \qquad [\mathrm{div}^c\,\mathbf{b},f]_\mathcal{F} = [\mathbf{b},\mathrm{div}^{c*}f]_\mathcal{E}, \tag{43b}$$

for any $\phi \in \mathcal{V}$, $\mathbf{b} \in \mathcal{E}$, $f \in \mathcal{F}$ [*plus boundary terms?*]. Derived operators (denoted with tildes, following the terminology and approach of [11]) are defined in terms of adjoint operators by

$$\widetilde{\text{grad}}^{v} = -\text{div}^{c*}, \quad \widetilde{\text{curl}}^{v} = \text{curl}^{v*}, \quad \widetilde{\text{curl}}^{c} = \text{curl}^{c*}, \quad \widetilde{\text{div}}^{c} = -\text{grad}^{v*}. \tag{44}$$

It follows from (38, 43) that the derived operators have the following matrix representations:

$$\widetilde{\text{grad}}^{v} = -(\mathsf{M}^{\mathcal{E}})^{-1}\text{div}^{c\top}\mathsf{M}^{\mathcal{F}}, \qquad \widetilde{\text{curl}}^{c} = (\mathsf{M}^{\mathcal{E}})^{-1}\text{curl}^{c\top}\mathsf{M}^{\mathcal{F}}, \tag{45a}$$

$$\widetilde{\text{curl}}^{v} = (\mathsf{M}^{\mathcal{V}})^{-1}\text{curl}^{v\top}\mathsf{M}^{\mathcal{E}}, \qquad \widetilde{\text{div}}^{c} = -(\mathsf{M}^{\mathcal{V}})^{-1}\text{grad}^{v\top}\mathsf{M}^{\mathcal{E}}. \tag{45b}$$

These relationships can be summarised as follows:

$$\begin{array}{ccccc} \mathcal{V} & \xrightarrow{\text{grad}^v} & \mathcal{E} & \xrightarrow{\text{curl}^c} & \mathcal{F} \\ \uparrow{\scriptstyle \mathsf{M}^{\mathcal{V}}} & & \uparrow{\scriptstyle \mathsf{M}^{\mathcal{E}}} & & \uparrow{\scriptstyle \mathsf{M}^{\mathcal{F}}} \\ \mathcal{V} & \xleftarrow[-\widetilde{\text{div}}^c]{} & \mathcal{E} & \xleftarrow[\widetilde{\text{curl}}^c]{} & \mathcal{F} \end{array} \quad \text{and} \quad \begin{array}{ccccc} \mathcal{V} & \xrightarrow{\text{curl}^v} & \mathcal{E} & \xrightarrow{\text{div}^c} & \mathcal{F} \\ \uparrow{\scriptstyle \mathsf{M}^{\mathcal{V}}} & & \uparrow{\scriptstyle \mathsf{M}^{\mathcal{E}}} & & \uparrow{\scriptstyle \mathsf{M}^{\mathcal{F}}} \\ \mathcal{V} & \xleftarrow[\widetilde{\text{curl}}^v]{} & \mathcal{E} & \xleftarrow[-\widetilde{\text{grad}}^v]{} & \mathcal{F} \end{array} . \tag{45c}$$

Under (45), $\widetilde{\text{div}}^{c} \circ \widetilde{\text{curl}}^{c} = 0$ and $\widetilde{\text{curl}}^{v} \circ \widetilde{\text{grad}}^{v} = 0$ are both satisfied exactly: for example,

$$\begin{aligned} -\widetilde{\text{div}}^{c} \circ \widetilde{\text{curl}}^{c} =& (\mathsf{M}^{\mathcal{V}})^{-1}(\text{grad}^{v})^{\top}\mathsf{M}^{\mathcal{E}} \circ (\mathsf{M}^{\mathcal{E}})^{-1}(\text{curl}^{c})^{\top}\mathsf{M}^{\mathcal{F}} \\ =& (\mathsf{M}^{\mathcal{V}})^{-1}((\mathsf{N}^{\mathcal{E}})^{-1}\mathsf{A}\mathsf{N}^{\mathcal{V}})^{\top}((\mathsf{N}^{\mathcal{F}})^{-1}\mathsf{B}\mathsf{N}^{\mathcal{E}})^{\top}\mathsf{M}^{\mathcal{F}} \\ =& (\mathsf{M}^{\mathcal{V}})^{-1}(\mathsf{N}^{\mathcal{V}})^{\top}\mathsf{A}^{\top}\mathsf{B}^{\top}((\mathsf{N}^{\mathcal{F}})^{-1})^{\top}\mathsf{M}^{\mathcal{F}}, \end{aligned} \tag{46}$$

which vanishes because $(\mathsf{B}\mathsf{A})^{\top} = \mathsf{0}$. The sequences in (45c) are therefore 'exact.'

Derived operators under the choice of inner product (38) are

$$\{\widetilde{\text{grad}}^{v} f\}_j = \textstyle\sum_i B_{ij} \dfrac{(\boldsymbol{\epsilon}_i \mathbf{t}_j)}{F_j} f_i, \qquad \{\widetilde{\text{curl}}^{c} f\}_j = \textstyle\sum_i B_{ij} \dfrac{\mathbf{t}_j}{F_j} f_i, \tag{47a}$$

$$\{\widetilde{\text{curl}}^{v} \mathbf{b}\}_k = \dfrac{1}{E_k}\textstyle\sum_j A_{jk} \dfrac{F_j}{t_j^2}(\boldsymbol{\epsilon}_k \mathbf{t}_j) \cdot \mathbf{b}_j, \qquad \{\widetilde{\text{div}}^{c} \mathbf{b}\}_k = -\dfrac{1}{E_k}\textstyle\sum_j A_{jk} \dfrac{F_j}{t_j^2} \mathbf{t}_j \cdot \mathbf{b}_j. \tag{47b}$$

It follows from (47) that grad^{v} and $\widetilde{\text{curl}}^{c}$ are both parallel to $\mathbf{t}_j$ and curl^{v} and $\widetilde{\text{grad}}^{v}$ are both parallel to $\boldsymbol{\epsilon}_i \mathbf{t}_j$.

By specifying fields appropriately in (43), we can write, for any $\phi \in \mathcal{V}$, $\mathbf{b} \in \mathcal{E}$ and $f \in \mathcal{V}$,

$$0 \leq [\text{grad}^{v}\,\phi, \text{grad}^{v}\,\phi]_{\mathcal{E}} = [\phi, -\widetilde{\text{div}}^{c} \circ \text{grad}^{v}\,\phi]_{\mathcal{V}}, \qquad 0 \leq [\text{curl}^{c}\,\mathbf{b}, \text{curl}^{c}\,\mathbf{b}]_{\mathcal{F}} = [\mathbf{b}, \widetilde{\text{curl}}^{c} \circ \text{curl}^{c}\,\mathbf{b}]_{\mathcal{E}}, \tag{48a}$$

$$0 \leq [\text{curl}^{v}\,\phi, \text{curl}^{v}\,\phi]_{\mathcal{E}} = [\phi, \widetilde{\text{curl}}^{v} \circ \text{curl}^{v}\,\phi]_{\mathcal{V}}, \qquad 0 \leq [\text{div}^{c}\,\mathbf{b}, \text{div}^{c}\,\mathbf{b}]_{\mathcal{F}} = [\mathbf{b}, -\widetilde{\text{grad}}^{v} \circ \text{div}^{c}\,\mathbf{b}]_{\mathcal{E}}, \tag{48b}$$

$$0 \leq [\widetilde{\text{grad}}^{v} f, \widetilde{\text{grad}}^{v} f]_{\mathcal{E}} = [f, -\text{div}^{c} \circ \widetilde{\text{grad}}^{v} f]_{\mathcal{F}}, \qquad 0 \leq [\widetilde{\text{curl}}^{v} \mathbf{b}, \widetilde{\text{curl}}^{v} \mathbf{b}]_{\mathcal{V}} = [\mathbf{b}, \text{curl}^{v} \circ \widetilde{\text{curl}}^{v} \mathbf{b}]_{\mathcal{E}}, \tag{48c}$$

$$0 \leq [\widetilde{\text{curl}}^{c} f, \widetilde{\text{curl}}^{c} f]_{\mathcal{E}} = [f, \text{curl}^{c} \circ \widetilde{\text{curl}}^{c} f]_{\mathcal{F}}, \qquad 0 \leq [\widetilde{\text{div}}^{c} \mathbf{b}, \widetilde{\text{div}}^{c} \mathbf{b}]_{\mathcal{V}} = [\mathbf{b}, -\text{grad}^{v} \circ \widetilde{\text{div}}^{c} \mathbf{b}]_{\mathcal{E}}. \tag{48d}$$

This construction identifies two positive-definite scalar Laplacians acting on $\mathcal{V}$,

$$-\widetilde{\text{div}}^{c} \circ \text{grad}^{v} = (\mathsf{M}^{\mathcal{V}})^{-1}(\mathsf{N}^{\mathcal{V}})^{\top}\mathsf{A}^{\top}(\mathsf{N}^{\mathcal{E}})^{-1,\top}\mathsf{M}^{\mathcal{E}}(\mathsf{N}^{\mathcal{E}})^{-1}\mathsf{A}\mathsf{N}^{\mathcal{V}} \tag{49a}$$

$$\widetilde{\text{curl}}^{v} \circ \text{curl}^{v} = (\mathsf{M}^{\mathcal{V}})^{-1}(\mathsf{N}^{\mathcal{V}})^{\top}\mathsf{A}^{\top}(\tilde{\mathsf{N}}^{\mathcal{E}})^{-1,\top}\mathsf{M}^{\mathcal{E}}(\tilde{\mathsf{N}}^{\mathcal{E}})^{-1}\mathsf{A}\mathsf{N}^{\mathcal{V}}, \tag{49b}$$

which differ in having at their heart $\hat{\mathbf{t}}_j^{\top}\{\mathsf{M}^{\mathcal{E}}\}_{jj}\hat{\mathbf{t}}_j$ and $(-\boldsymbol{\epsilon}_i\hat{\mathbf{t}}_j)^{\top}\{\mathsf{M}^{\mathcal{E}}\}_{jj}(-\boldsymbol{\epsilon}_k\hat{\mathbf{t}}_j)$. Taking $\mathsf{M}^{\mathcal{E}} = \text{diag}(\mathsf{I}F_j)$ recovers $\mathsf{L}_{\mathcal{V}}$ (see (9a)) in each case in (49). There are two positive-definite scalar Laplacians acting on $\mathcal{F}$, which for $\mathsf{M}^{\mathcal{E}} = \text{diag}(\mathsf{I}F_j)$ reduce to

$$-\text{div}^{c} \circ \widetilde{\text{grad}}^{v} = \mathsf{L}_{\mathcal{F}}, \quad \text{curl}^{c} \circ \widetilde{\text{curl}}^{c} = \mathsf{L}_{\mathcal{F}}. \tag{49c}$$

We also identify four positive-definite vector Laplacians acting on $\mathcal{E}$, including

$$-\widetilde{\text{grad}}^{\,v} \circ \text{div}^c = (\mathsf{M}^{\mathcal{E}})^{-1}(\tilde{\mathsf{N}}^{\mathcal{E}})^\top \mathsf{B}^\top (\mathsf{N}^{\mathcal{F}})^{-1,\top} \mathsf{M}^{\mathcal{F}} (\mathsf{N}^{\mathcal{F}})^{-1} \mathsf{B}\tilde{\mathsf{N}}^{\mathcal{E}}, \tag{50a}$$

$$\widetilde{\text{curl}}^{\,c} \circ \text{curl}^c = (\mathsf{M}^{\mathcal{E}})^{-1}(\mathsf{N}^{\mathcal{E}})^\top \mathsf{B}^\top (\mathsf{N}^{\mathcal{F}})^{-1,\top} \mathsf{M}^{\mathcal{F}} (\mathsf{N}^{\mathcal{F}})^{-1} \mathsf{B}\mathsf{N}^{\mathcal{E}}. \tag{50b}$$

We can also use (43) to obtain the orthogonality relations

$$[\text{grad}^v \phi, \widetilde{\text{curl}}^{\,c} f]_{\mathcal{E}} = 0 \quad \text{and} \quad [\text{curl}^v \phi, \widetilde{\text{grad}}^{\,v} f]_{\mathcal{E}} = 0, \tag{51}$$

which hold for any functions $\phi \in \mathcal{V}$ and $f \in \mathcal{F}$. These results rely on $\mathsf{BA} = \mathsf{0}$, rather than geometric orthogonality. This leads to the decomposition given in (10).

[*Results in [11] suggest that* $\ker(\text{grad}^v)$ *is the set of constant vectors in* $\mathcal{V}$, $\ker(\text{curl}^c) = \text{im}(\text{grad}^v)$, $\ker(\text{div}^c) = \text{im}(\text{curl}^v)$*, with analogous results for derived operators.*]

A.2 Operators on the dual network

Primary operators on the dual network are defined as follows:

$$\begin{array}{ccccc} \mathcal{T} & \xleftarrow{\text{CURL}^v} & \mathcal{L} & \xleftarrow{\text{grad}^c} & \mathcal{C} \\ \downarrow{\scriptstyle \mathsf{N}^{\mathcal{T}}} & & \downarrow{\scriptstyle \mathsf{N}^{\mathcal{L}}} & & \downarrow{\scriptstyle \mathsf{N}^{\mathcal{C}}} \\ \mathcal{T} & \xleftarrow{\mathsf{A}^\top} & \mathcal{L} & \xleftarrow{\mathsf{B}^\top} & \mathcal{C} \end{array} \quad \text{and} \quad \begin{array}{ccccc} \mathcal{T} & \xleftarrow{\text{div}^v} & \mathcal{L} & \xleftarrow{\text{CURL}^c} & \mathcal{C} \\ \downarrow{\scriptstyle \mathsf{N}^{\mathcal{T}}} & & \downarrow{\scriptstyle \tilde{\mathsf{N}}^{\mathcal{L}}} & & \downarrow{\scriptstyle \mathsf{N}^{\mathcal{C}}} \\ \mathcal{T} & \xleftarrow{\mathsf{A}^\top} & \mathcal{L} & \xleftarrow{\mathsf{B}^\top} & \mathcal{C} \end{array} . \tag{52}$$

Here $\mathsf{N}^{\mathcal{C}} = \mathsf{I}$, $\mathsf{N}^{\mathcal{L}} = \text{diag}(\mathbf{T}_j^\top)$, $\tilde{\mathsf{N}}^{\mathcal{L}} = \text{diag}(-(\boldsymbol{\epsilon}_k \mathbf{T}_j)^\top)$, $\mathsf{N}^{\mathcal{T}} = \text{diag}(E_k)$. $\mathcal{T}$, $\mathcal{L}$ and $\mathcal{C}$ are vector spaces of fields defined over triangles, links and cell centres. We can make the association $\mathcal{T} = \mathcal{V}$, $\mathcal{L} = \mathcal{E}$, $\mathcal{C} = \mathcal{F}$ (subject to boundary effects). Derived operators are defined using the inner products with metrics $\mathsf{M}^{\mathcal{T}} = \mathsf{M}^{\mathcal{V}}$, $\mathsf{M}^{\mathcal{L}} = \mathsf{M}^{\mathcal{E}}$, $\mathsf{M}^{\mathcal{C}} = \mathsf{M}^{\mathcal{F}}$, via

$$\begin{array}{ccccc} \mathcal{T} & \xleftarrow{\text{CURL}^v} & \mathcal{L} & \xleftarrow{\text{grad}^c} & \mathcal{C} \\ \uparrow{\scriptstyle \mathsf{M}^{\mathcal{T}}} & & \uparrow{\scriptstyle \mathsf{M}^{\mathcal{L}}} & & \uparrow{\scriptstyle \mathsf{M}^{\mathcal{C}}} \\ \mathcal{T} & \xrightarrow[\widetilde{\text{CURL}}^{\,v}]{} & \mathcal{L} & \xrightarrow[-\widetilde{\text{div}}^{\,v}]{} & \mathcal{C} \end{array} \quad \text{and} \quad \begin{array}{ccccc} \mathcal{T} & \xleftarrow{\text{div}^v} & \mathcal{L} & \xleftarrow{\text{CURL}^c} & \mathcal{C} \\ \uparrow{\scriptstyle \mathsf{M}^{\mathcal{T}}} & & \uparrow{\scriptstyle \mathsf{M}^{\mathcal{L}}} & & \uparrow{\scriptstyle \mathsf{M}^{\mathcal{C}}} \\ \mathcal{T} & \xrightarrow[-\widetilde{\text{grad}}^{\,c}]{} & \mathcal{L} & \xrightarrow[\widetilde{\text{CURL}}^{\,c}]{} & \mathcal{C} \end{array} . \tag{53}$$

Thus

$$\{\text{grad}^c f\}_j = \textstyle\sum_i B_{ij} \dfrac{\mathbf{T}_j}{T_j^2} f_i, \qquad \{\text{CURL}^v \mathbf{b}\}_k = \dfrac{1}{E_k} \textstyle\sum_j A_{jk} \mathbf{T}_j \cdot \mathbf{b}_j, \tag{54a}$$

$$\{\text{CURL}^c f\}_j = \textstyle\sum_k \dfrac{\boldsymbol{\epsilon}_i \mathbf{T}_j}{T_j^2} B_{ij} f_i, \qquad \{\text{div}^v \mathbf{b}\}_k = -\dfrac{1}{E_k} \textstyle\sum_j A_{jk} (\boldsymbol{\epsilon}_k \mathbf{T}_j) \cdot \mathbf{b}_j \tag{54b}$$

and [*check signs, transposes*]

$$\{\widetilde{\text{grad}}^{\,c} \phi\}_j = \textstyle\sum_k A_{jk} \dfrac{(\boldsymbol{\epsilon}_k \mathbf{T}_j)}{F_j} \phi_k \qquad \{\widetilde{\text{CURL}}^{\,v} \phi\}_j = \dfrac{1}{F_j} \textstyle\sum_j A_{jk} \mathbf{T}_j \phi_k \tag{55a}$$

$$\{\widetilde{\text{CURL}}^{\,c} \mathbf{b}\}_i = \dfrac{1}{E_k} \textstyle\sum_j B_{ij} \dfrac{{F_j}^2}{T_j} (\boldsymbol{\epsilon}_i \mathbf{T}_j) \cdot \mathbf{b}_j \qquad \{\widetilde{\text{div}}^{\,v} \mathbf{b}\}_i = -\dfrac{1}{A_i} \textstyle\sum_j B_{ij} \dfrac{F_j}{T_j^2} \mathbf{T}_j \cdot \mathbf{b}_j \tag{55b}$$

The primary and derived operators over the two networks then act as shown below:

$$\begin{array}{ccc} \mathcal{V} & \xleftarrow{\mathsf{M}^{\mathcal{V}}} & \mathcal{V} \\ {\scriptstyle \text{curl}^v}\downarrow \quad {\scriptstyle \text{grad}^v} & & {\scriptstyle \widetilde{\text{curl}}^{\,v}}\uparrow \quad {\scriptstyle -\widetilde{\text{div}}^{\,c}} \\ \mathcal{E} & \xleftarrow{\mathsf{M}^{\mathcal{E}}} & \mathcal{E} \\ {\scriptstyle \text{div}^c}\downarrow \quad {\scriptstyle \text{curl}^c} & & {\scriptstyle -\widetilde{\text{grad}}^{\,v}}\uparrow \quad {\scriptstyle \widetilde{\text{curl}}^{\,c}} \\ \mathcal{F} & \xleftarrow{\mathsf{M}^{\mathcal{F}}} & \mathcal{F} \end{array} \qquad \begin{array}{ccc} \mathcal{T} & \xleftarrow{\mathsf{M}^{\mathcal{T}}} & \mathcal{T} \\ {\scriptstyle \text{CURL}^v}\uparrow \quad {\scriptstyle \text{div}^v} & & {\scriptstyle \widetilde{\text{CURL}}^{\,v}}\downarrow \quad {\scriptstyle -\widetilde{\text{grad}}^{\,c}} \\ \mathcal{L} & \xleftarrow{\mathsf{M}^{\mathcal{L}}} & \mathcal{L} \\ {\scriptstyle \text{grad}^c}\uparrow \quad {\scriptstyle \text{CURL}^c} & & {\scriptstyle -\widetilde{\text{div}}^{\,v}}\downarrow \quad {\scriptstyle \widetilde{\text{CURL}}^{\,c}} \\ \mathcal{C} & \xleftarrow{\mathsf{M}^{\mathcal{C}}} & \mathcal{C} \end{array} . \tag{56}$$

This leads to the Helmholtz decomposition given in (12).

A.3 Operators acting on tensors

Divergence of quantities $\boldsymbol{\sigma}$ defined on vertices or cell centres is given by

$$\{\mathrm{div}^c \boldsymbol{\sigma}^c\} = \textstyle\sum_j \boldsymbol{\epsilon}_i^\top B_{ij} \mathbf{t}_j \cdot \boldsymbol{\sigma}_i / A_i = A_i^{-1} \sum_j \mathbf{n}_{ij} \cdot \boldsymbol{\sigma}_i \tag{57a}$$

$$\{\mathrm{div}^v \boldsymbol{\sigma}^v\} = \textstyle\sum_j \boldsymbol{\epsilon}_k^\top A_{jk} \mathbf{T}_j \cdot \boldsymbol{\sigma}_k / E_k = E_k^{-1} \sum_j \mathbf{N}_{jk} \cdot \boldsymbol{\sigma}_k \tag{57b}$$

Divergence maps from cells/faces to links/edges [*not clear via notation*].

B Changes of area and perimeter under non-uniform deformations

Here we consider how area and perimeter change under deformations $\mathbf{u}(\mathbf{x})$ that vary with position, over length-scales long compared to an individual cell. Dropping third (and higher) spatial derivatives of $\mathbf{u}$, edges, edge lengths and normals map under the deformation to

$$\mathbf{t}_j \equiv \textstyle\sum_k A_{jk} \mathbf{r}_k = \mathbf{t}'_j + \sum_k A_{jk} \mathbf{u}(\mathbf{r}'_k) = \mathbf{t}'_j + \mathbf{t}'_j \cdot (\nabla \mathbf{u})_j + \ldots, \tag{58a}$$

$$t_j \equiv \sqrt{\mathbf{t}_j \cdot \mathbf{t}_j} = t'_j \left[1 + \hat{\mathbf{t}}'_j \cdot \mathsf{E}_j \cdot \hat{\mathbf{t}}'_j + \ldots\right], \tag{58b}$$

$$\mathbf{n}_{ij} \equiv -\boldsymbol{\epsilon}_i B_{ij} \mathbf{t}_j = \mathbf{n}'_{ij} + \mathbf{n}'_{ij} \cdot (\nabla \mathbf{u})_j + \cdots = \mathbf{n}'_{ij} \cdot \left[\mathsf{I} + (\nabla \mathbf{u})_i + \mathbf{v}'_{ij} \cdot \mathsf{M}_i\right] + \ldots, \tag{58c}$$

where (58c) shows how the mapping is referred to an adjacent cell centre. Here $\mathbf{v}_{ij}$ is the vector connecting cell centre $\mathbf{R}_i$ to an adjacent edge centroid $\mathbf{c}_j$, i.e. $\overline{B}_{ij}(\mathbf{c}_j - \mathbf{R}_i - \mathbf{v}_{ij}) = \mathbf{0}$. We define the cell centre to be the centroid with respect to vertices, i.e. $\mathbf{R}_i = Z_i^{-1} \sum_k C_{ik} \mathbf{r}_k$. It is also the centroid relative to edge centroids (because $\sum_k C_{ik} \mathbf{r}_k = \frac{1}{2} \sum_{jk} \overline{B}_{ij} \overline{A}_{jk} \mathbf{r}_k = \sum_j \overline{B}_{ij} \mathbf{c}_j$, ensuring that $\sum_j \overline{B}_{ij} \mathbf{v}_{ij} = \mathbf{0}$). Likewise

$$\mathsf{E}_j = \mathsf{E}_i + \mathbf{v}'_{ij} \cdot (\nabla \mathsf{E})_i + \ldots \tag{59}$$

Edge centroids map to

$$\mathbf{c}_j = \mathbf{c}'_j + \mathbf{u}_j + \tfrac{1}{8} (\mathbf{t}'_j \cdot \nabla)(\mathbf{t}'_j \cdot \nabla) \mathbf{u}|_j + \cdots = \mathbf{c}'_j + \mathbf{u}_j + \tfrac{1}{8} (\mathbf{t}'_j \otimes \mathbf{t}'_j) : \mathsf{M}_j + \ldots. \tag{60}$$

Using $\mathbf{R}_i = Z_i^{-1} \sum_j \overline{B}_{ij} \mathbf{c}_j$, cell centres map to

$$\mathbf{R}_i = \mathbf{R}'_i + \mathbf{u}_i + \tfrac{1}{2} \mathsf{V}_i : \mathsf{M}_i + \tfrac{1}{8} \mathsf{T}_i : \mathsf{M}_i + \ldots \tag{61}$$

where $\mathsf{V}_i \equiv Z_i^{-1} \sum_j \overline{B}_{ij} \mathbf{v}'_{ij} \otimes \mathbf{v}'_{ij}$ (arising from averaging displacements around the edges of the cell) and $\mathsf{T}_i \equiv Z_i^{-1} \sum_j \overline{B}_{ij} \mathbf{t}'_j \otimes \mathbf{t}'_j$. Combining (60) and (61), links from cell centres to edge centroids map to

$$\mathbf{v}_{ij} = \mathbf{v}'_{ij} + \mathbf{v}'_{ij} \cdot (\nabla \mathbf{u})_i + \left[\tfrac{1}{2} (\mathbf{v}'_{ij} \otimes \mathbf{v}'_{ij}) - \tfrac{1}{2} \mathsf{V}_i + \tfrac{1}{8} \overline{B}_{ij} (\mathbf{t}'_j \otimes \mathbf{t}'_j) - \tfrac{1}{8} \mathsf{T}_i\right] : \mathsf{M}_i + \ldots \tag{62}$$

Using (60) and (58b), cell perimeters change according to

$$L_i \equiv \sum_j \overline{B}_{ij} t_j = L'_i (1 + \mathsf{Q}_i : \mathsf{E}_i) + \textstyle\sum_j \overline{B}_{ij} t'_j \hat{\mathbf{t}}'_j \cdot \left[\mathbf{v}'_{ij} \cdot (\nabla \mathsf{E})_i\right] \cdot \hat{\mathbf{t}}'_j + \ldots, \tag{63}$$

where $L'_i \mathsf{Q}_i \equiv \sum_j \overline{B}_{ij} \mathbf{t}'_j \otimes \hat{\mathbf{t}}'_j$. Writing the final term as $L'_i \mathsf{X}_i \vdots (\nabla \mathsf{E})_i$ reveals the 3-tensor X_i characterising the impact of strain gradients on cell perimeter. W does not affect perimeter changes to this order.

Using (58c) and (62), the cell area becomes

$$\begin{aligned} A_i \equiv & \tfrac{1}{2} \textstyle\sum_j \mathbf{n}_{ij} \cdot \mathbf{v}_{ij} \\ = & A'_i + \textstyle\sum_j \left\{ \mathbf{v}'_{ij} \cdot \mathsf{E}_i \cdot \mathbf{n}'_{ij} + \tfrac{1}{2} \left[\mathbf{n}'_{ij} \cdot (\mathbf{v}'_{ij} \cdot \mathsf{M}_i)\right] \cdot \mathbf{v}'_{ij} + \tfrac{1}{2} \left(\left[\tfrac{1}{2} \mathbf{v}'_{ij} \otimes \mathbf{v}'_{ij} + \tfrac{1}{8} \overline{B}_{ij} \mathbf{t}'_j \otimes \mathbf{t}'_j - \tfrac{1}{2} \mathsf{V}_i - \tfrac{1}{8} \mathsf{T}_i \right] : \mathsf{M}_i \right) \cdot \mathbf{n}'_{ij} \right\}. \end{aligned}$$

Note that

$$\textstyle\sum_j \mathbf{n}_{ij}\otimes\mathbf{v}_{ij} = \sum_j \mathbf{n}_{ij}\otimes\mathbf{c}_{ij} = \oint_i \mathbf{x}\hat{\mathbf{n}}\,\mathrm{d}s = \int_i \nabla\mathbf{x}\,\mathrm{d}A = A_i\mathsf{I}. \tag{64}$$

A similar argument gives

$$\textstyle\left(\sum_j \mathbf{n}_{ij}\otimes\mathbf{v}_{ij}\otimes\mathbf{v}_{ij}\right)_{pqr} \equiv \sum_j n_{ij,p}v_{ij,q}v_{ij,r} = A_i\left[\delta_{pq}(\rho_{i,r}-R_{i,r})+\delta_{pr}(\rho_{i,q}-R_{i,q})\right] \tag{65}$$

where $\boldsymbol{\rho}_i \equiv A_i^{-1}\int_i \mathbf{x}\,\mathrm{d}A$ is the area-centroid of the cell, which in general will be distinct from the vertex centroid $\mathbf{R}_i$. Thus

$$\left[\mathbf{n}'_{ij}\cdot(\mathbf{v}'_{ij}\cdot\mathsf{M}_i)\right]\cdot\mathbf{v}'_{ij} = A'_i(\boldsymbol{\rho}'_i-\mathbf{R}'_i)\cdot[\nabla^2\mathbf{u}_i+\nabla(\nabla\cdot\mathbf{u}_i)] \equiv 2A'_i(\boldsymbol{\rho}'_i-\mathbf{R}'_i)\cdot[\mathsf{I}:\nabla\mathsf{E}]_i \tag{66a}$$

$$\left(\left[\mathbf{v}'_{ij}\otimes\mathbf{v}'_{ij}\right]:\mathsf{M}_i\right)\cdot\mathbf{n}'_{ij} = 2A'_i(\boldsymbol{\rho}'_i-\mathbf{R}'_i)\cdot\nabla(\nabla\cdot\mathbf{u}_i) \equiv 2A'_i(\boldsymbol{\rho}'_i-\mathbf{R}'_i)\cdot[\nabla(\mathsf{I}:\mathsf{E})]_i \tag{66b}$$

This gives

$$A_i = A'_i\left[1+\mathsf{I}:\mathsf{E}_i+(\boldsymbol{\rho}'_i-\mathbf{R}'_i)\cdot[\mathsf{I}:\nabla\mathsf{E}]_i+\tfrac{1}{2}(\boldsymbol{\rho}'_i-\mathbf{R}'_i)\cdot[\nabla(\mathsf{I}:\mathsf{E})]_i\right]+\tfrac{1}{2}\textstyle\sum_j\left(\left[\frac{1}{8}\overline{B}_{ij}\mathbf{t}'_j\otimes\mathbf{t}'_j\right]:\mathsf{M}_i\right)\cdot\mathbf{n}'_{ij}.$$

As $\mathbf{R}_i$ is the cell centroid (relative to vertices) then $\sum_j \mathbf{v}'_{ij}=\mathbf{0}$ and $\sum_j \mathbf{n}'_{ij}=\mathbf{0}$. [*Check: consider how a different choice of centroid eliminates the second and third terms.*] Then we note that

$$\begin{aligned}
t_{j,p}t_{j,q}n_{ij,r}M_{pqr} &= -B_{ij}t_{j,p}t_{j,q}\epsilon_{i,rs}t_{j,s}(\partial_pE_{qr}+\partial_pW_{qr}) = -B_{ij}t_{j,p}t_{j,q}\epsilon_{i,rs}t_{j,s}(\partial_pE_{qr}+\partial_p\varepsilon_{qr}\omega_i)\\
&= \mp B_{ij}t_{j,p}t_{j,q}\varepsilon_{rs}t_{j,s}(\partial_pE_{qr}+\partial_p\varepsilon_{qr}\omega_i) = \mp B_{ij}t_{j,p}t_{j,q}t_{j,s}(\varepsilon_{rs}\partial_pE_{qr}-\delta_{qs}\partial_p\omega_i)\\
&= \mp B_{ij}t_{j,p}(t_{j,q}t_{j,s}\varepsilon_{rs}\partial_pE_{qr}-l_j^2\partial_p\omega_i) = \mp B_{ij}t_{j,p}t_{j,q}t_{j,s}\varepsilon_{rs}\partial_pE_{qr}+2l_j^2\mathbf{n}_{ij}\cdot\boldsymbol{\kappa}_i
\end{aligned} \tag{67}$$

taking $\boldsymbol{\epsilon}_i = \pm\boldsymbol{\varepsilon}$ and noting that $\mathbf{n}_{ij}\cdot\boldsymbol{\kappa}_i = \pm\frac{1}{2}B_{ij}t_{j,p}\partial_p\omega_i$.

Hence, with this constraint on cell centre location, we can write

$$A_i = A'_i\left[1+\mathsf{I}:\mathsf{E}_i+\mathsf{Y}_i\vdots(\nabla\mathsf{E})_i+\left[\frac{1}{8A'_i}\textstyle\sum_j\overline{B}_{ij}(t'_j)^2\mathbf{n}'_{ij}\right]\cdot\boldsymbol{\kappa}_i\right] \tag{68}$$

where Y_i has dimensions of length.

C Stress over the dual network

The energy in (30) is partitioned across cells, but it can be reoorganised to be partitioned over kites. The cell area A_i can be partitioned into kite areas K_{ik} so that $A_i=\sum_k K_{ik}$ and $\hat{E}_k=\sum_i K_{ik}$. The leading-order force-stress contribtution to the energy can be written

$$\textstyle\sum_i A_i\boldsymbol{\sigma}_i^{(s)}:\mathsf{E}_i \equiv \sum_i(A_i\mathcal{P}_i\mathsf{I}+\mathcal{T}_iL_i\mathsf{Q}_i):\mathsf{E}_i = \sum_k\hat{E}_k\boldsymbol{\sigma}_k^{(s)}:\mathsf{E}_k \tag{69}$$

Likewise we can write

$$L_i\mathsf{Q}_i \equiv \textstyle\sum_j\overline{B}_{ij}\mathbf{t}_j\otimes\hat{\mathbf{t}}_j = \sum_{j,k}\frac{1}{2}\overline{B}_{ij}\mathbf{t}_j\otimes\hat{\mathbf{t}}_j\overline{A}_{jk}. \tag{70}$$

To leading order, strain gradients can be neglected and we may assume $\overline{C}_{ik}(\mathsf{E}_k-\mathsf{E}_i)=\mathsf{0}$. Then the symmetric force stress over a tristar is given by

$$\hat{E}_k\boldsymbol{\sigma}_k = \textstyle\sum_i\left[K_{ik}\mathcal{P}_i\mathsf{I}+\frac{1}{2}\mathcal{T}_i\sum_j\overline{B}_{ij}\mathbf{t}_j\otimes\hat{\mathbf{t}}_j\overline{A}_{jk}\right]. \tag{71}$$

Taking the trace gives the isotropic stress over a tristar as

$$P_{\mathrm{eff},k} = \sum_i\left[\frac{K_{ik}\mathcal{P}_i}{\hat{E}_k}+\frac{1}{4\hat{E}_k}\mathcal{T}_i\textstyle\sum_j\overline{B}_{ij}t_j\overline{A}_{jk}\right]. \tag{72}$$

The deviatoric stress is symmetric, and is

$$\check{\boldsymbol{\sigma}}_k = \frac{1}{2\hat{E}_k} \sum_{i,j} \mathcal{T}_i \overline{B}_{ij} t_j (\hat{\mathbf{t}}_j \otimes \hat{\mathbf{t}}_j - \tfrac{1}{2}\mathsf{I}) \overline{A}_{jk}. \tag{73}$$

The micoscopic stress over the tristar is

$$\hat{E}_k \tilde{\boldsymbol{\sigma}}_k = \cup_i \left[K_{ik} \mathcal{P}_i \mathsf{I} + \tfrac{1}{2} \mathcal{T}_i \cup_j \overline{B}_{ij} \mathbf{t}_j \otimes \hat{\mathbf{t}}_j \overline{A}_{jk} \right]. \tag{74}$$

[*Show that* $\mathrm{div}^t \tilde{\boldsymbol{\sigma}}_k = \mathbf{0}$*, where* div^t *is a divergence over tristars rather than triangles. Break the integral into divergence over each kite, and recover force balance over vertex* k*.*]

[*Consider alternative formulations over triangles, rather than tristars.*]

In general, we do not expect $\mathrm{div}^v \boldsymbol{\sigma}_k$ to vanish, whether or not it is defined over triangles or tristars.

References

[1] T. Nagai and H. Honda. A dynamic cell model for the formation of epithelial tissues. *Phil. Mag. B*, 81:699–719, 2001.

[2] R. Farhadifar, J.-C. Röper, B. Aigouy, S. Eaton, and F. Jülicher. The influence of cell mechanics, cell-cell interactions, and proliferation on epithelial packing. *Curr. Biol.*, 17:2095–2104, 2007.

[3] A. G. Fletcher, M. Osterfield, R. E. Baker, and S. Y. Shvartsman. Vertex models of epithelial morphogenesis. *Biophys. J.*, 106:2291–2304, 2014.

[4] S. Alt, P. Ganguly, and G. Salbreux. Vertex models: from cell mechanics to tissue morphogenesis. *Phil. Trans. R. Soc. B*, 372(1720):20150520, 2017.

[5] S. Ishihara, P. Marcq, and K. Sugimura. From cells to tissue: A continuum model of epithelial mechanics. *Phys. Rev. E*, 96(2):022418, 2017.

[6] A. Nestor-Bergmann, G. Goddard, S. Woolner, and O. E. Jensen. Relating cell shape and mechanical stress in a spatially disordered epithelium using a vertex-based model. *Math. Med. Biol.*, 35:1–27, 2018.

[7] A. Nestor-Bergmann, E. Johns, S. Woolner, and O. E. Jensen. Mechanical characterization of disordered and anisotropic cellular monolayers. *Phys. Rev. E*, 97:052409, May 2018.

[8] O. E. Jensen, E. Johns, and S. Woolner. Force networks, torque balance and Airy stress in the planar vertex model of a confluent epithelium. *Proc Roy Soc A*, 2020.

[9] R. D. Mindlin. Influence of couple-stresses on stress concentrations. Technical report, Columbia University, New York, 1962.

[10] A. R. Hadjesfandiari and G. F. Dargush. Couple stress theory for solids. *Int. J. Solids & Struct.*, 48(18):2496–2510, 2011.

[11] Lourenço Beirao da Veiga, Konstantin Lipnikov, and Gianmarco Manzini. *The mimetic finite difference method for elliptic problems*, volume 11. Springer, 2014.

[12] L. J. Grady and J. R. Polimeni. *Discrete calculus: Applied analysis on graphs for computational science.* Springer Science & Business Media, 2010.